Photoionization of the $3s^2 3p^4\ ^3P$ and the $3s^2 3p^4\ ^1D,\ ^1S$ states of sulfur: experiment and theory

Mathias Barthel[1],* Roman Flesch[1], and Eckart Rühl[1]†
[1] *Physikalische Chemie, Freie Universität Berlin, Takustr. 3, D-14195 Berlin, Germany*

Brendan M. McLaughlin[2,3]‡
[2] *Centre for Theoretical Atomic, Molecular and Optical Physics (CTAMOP), School of Mathematics and Physics, The David Bates Building, 7 College Park, Queen's University of Belfast, Belfast BT7 1NN, United Kingdom*
[3] *Institute for Theoretical Atomic and Molecular Physics, Harvard Smithsonian Center for Astrophysics, 60 Garden Street, MS-14, Cambridge, MA 02138, USA*

(Dated: January 15, 2015)

Photoionization of neutral atomic sulfur in the ground and metastable states was studied experimentally at a photon energy resolution of 44 meV FWHM. Relative cross section measurements were recorded by using tunable vacuum ultraviolet (VUV) radiation in the energy range 9 – 30 eV obtained from a laser-produced plasma and the atomic species were generated by photolysis of molecular precursors. Photoionization of this atom is characterized by multiple Rydberg series of autoionizing resonances superimposed on a direct photoionization continuum. A wealth of resonance features observed in the experimental spectra are spectroscopically assigned and their energies and quantum defects tabulated. The cross-section measurements are compared with state-of-the-art theoretical cross-section calculations obtained from the Dirac Coulomb *R*-matrix method. Resonances series in the spectra are identified and compared indicating similar features in both the theoretical and experimental spectra.

PACS numbers: 32.80.Fb, 32.80.Zb, 32.80.Ee

arXiv:1412.8715v2 [astro-ph.EP] 14 Jan 2015

I. INTRODUCTION

In astrophysics, abundance calculations are based on available atomic data that often are insufficient to make definite identifications of spectroscopic lines [1]. In planetary nebulae, the known emission lines are used to identify a characteristic element resulting from the process of nucleosynthesis in stars [2, 3]. The study of the photoionization of sulfur is of considerable interest because of its abundance in space and interstellar media. Sulfur has been discovered in the plasma of the Jupiter satellite Io and its occurrence in the solar atmosphere makes it of high astrophysical relevance [4–6]. It is known that Io is the source of Na, K, S, and O clouds observed in the near-Io spatial environment and in extended regions throughout the Jovian magnetosphere [7]. Spectroscopic measurements indicate that sulfur and oxygen dominate the torus plasma of the Jupiter satellite Io. Sulfur has also been discovered in Comet Comae as has CS with abundances of 10^{-3} of water [8]. Sulfur chemistry is also of importance in theoretical studies of interstellar shocks [9]. Photoabsorption and photoionization processes in the vacuum ultraviolet (VUV) region play an important role in determining solar and stellar opacities [10–12]. Determining accurate abundances for atomic sulfur is of great importance in understanding extragalactic H II regions [13].

The photoionization spectrum of sulfur has been studied in detail both theoretically and experimentally. On the experimental side, the sulfur absorption spectrum was reported by Tondello [14] for the energy regions below and above the ionization threshold. Absolute values of the cross section for the photoionization of the ground state ($3s^2 3p^4\ ^3P$) of sulfur for photon energies from the threshold at 119.67 nm to 90 nm (10.38 – 13.8 eV) using the flash-pyrolysis method, i.e. irradiating the sample with a strong flux of light from a discharge flash lamp. Sarma and Joshi [15] studied the photoionization spectrum of sulfur using a method similar to Tondello's. They modified and extended Tondello's spectrum, particularly in the region between 109 and 100 nm (11.39 – 12.42 eV). Gibson *et al.* [16] observed the photoionization spectrum of sulfur in the region between the first ionization threshold and 95 nm (13.05 eV). They found that the autoionization features of the $3s^2 3p^3(^2D^\circ)nd\ ^3D^\circ$ levels are broad while that of the $3s^2 3p^3(^2D^\circ)nd\ ^3S^\circ, ^3P^\circ$ levels are narrow. Their results are in good agreement with the measurements of Tondello. However, they reversed the designation given by Tondello to the $3s^2 3p^3(^2D^\circ)nd\ ^3S^\circ$ and $3s^2 3p^3(^2D^\circ)ns\ ^3D^\circ$ and supported these assignment of the levels mainly on the basis of the quantum defects of the two series. Experimental measurements published by Joshi *et al.* [17] contained the photoabsorption spectrum of sulfur in the wavelength 122 – 84 nm range (10.18 – 14.79 eV) giving a detailed comparison of the line list

* barthel@woelfel.de; Present address: Wölfel Beratende Ingenieure GmbH + Co. KG, Max-Planck-Str. 15, 97204 Höchberg, Germany
† Corresponding author: ruehl@zedat.fu-berlin.de
‡ Corresponding author: b.mclaughlin@qub.ac.uk

obtained in their measurement with that of Tondello [14], Sarma and Joshi [15], and Gibson *et al.* [16]. The emission spectrum of sulfur has been studied by a number of experimental groups in the energy regions below and above the first ionization limit. Kaufman [18] measured 114 lines of atomic sulfur in the wavelength region 216.9 – 115.7 nm (5.73 eV - 10.73 eV) involving transitions to the levels of the ground state configuration.

Recent experiments performed by Jackson and co-workers [19–22] measured the single-photon excitation spectra from the lowest $3s^2 3p^4\ ^1D_2$ and $3s^2 3p^4\ ^1S_0$ metastable levels of sulfur atoms recorded with a tunable vacuum ultraviolet (VUV) radiation source generated by frequency tripling in noble gases. Various new lines were observed in the spectra which have not been previously reported. The photoionization efficiency (PIE) spectra of metastable sulfur (S) atoms in the $(3s^2 3p^4\ ^1D_2)$ and $(3s^2 3p^4\ ^1S_0)$ states have been recorded in the 73 350 – 84 950 cm^{-1} frequency range (9.094 – 10.532 eV) by using a velocity-map ion imaging apparatus that uses a tunable VUV laser as an ionization source.

In experiments carried out by Pan and co-workers [23] they recorded the photoionization spectra of sulfur atoms in transitions from the $3s^2 3p^4\ ^1D_2$ state in the energy range of 75 800 – 89 500 cm^{-1} (9.4 - 11.1 eV). They recorded and assigned the Rydberg series $3s^2 3p^3(^2D^\circ_{3/2})nd[3/2]$ and $3s^2 3p^3(^2D^\circ_{3/2})nd[5/2]$ with n extending to 16 and 32, respectively, to the $^2D^\circ$ series limit. In addition, new Rydberg series $3s^2 3p^3(^2D^\circ_{3/2})nd[1/2]$, $3s^2 3p^3(^2D^\circ_{5/2})nd[5/2]$ and $3s^2 3p^3(^2D^\circ_{3/2})nd[5/2]$ with n ranging from 5 – 9 for the former two series and 7 – 13 for the latter were able to be assigned.

The present paper uses a technique that was applied to photoionization and autoionization of atomic singlet oxygen O(^{1}D) previously [24, 25]. Suitable photochemical precursors of electronically excited atomic or molecular species are photolyzed using a pulsed, tunable laser. Photodissociation products are subsequently photoionized using a pulsed, tunable VUV light source. Investigations are facilitated in systems where the primary photoproduct occurs in well-defined quantum states.

Carbon disulfide (CS_2) is used as a source of atomic sulfur in both the ^3P ground state and the first excited (^1D) metastable state. The ultraviolet photoabsorption cross section of CS_2 has been investigated previously [26–29]. Between 180 nm (6.89 eV) and 220 nm (5.64 eV) there is an intense band system that corresponds to the $X\ ^1\Sigma_g^+ \rightarrow\ ^1B_2(^1\Sigma_u^-)$ transition with photoabsorption cross sections as high as > 500 Mb for bands around 200 nm. The $^1B_2$ state is predissociated by (CS + S(^{3}P)) and a (CS + S(^{1}D)) continuous states. At 193 nm (6.424 eV) the photoabsorption cross section is estimated to be $\sigma \approx 290$ Mb using interpolated data reported in Ref. [29]. At this wavelength photolysis can be carried out conveniently by a pulsed ArF laser (see Section II).

Hence, atomic sulfur species S($3s^2 3p^4\ ^3P$) and S($3s^2 3p^4\ ^1D$) were received in mixture by photolysis of CS_2. The branching ratio of both species at 193 nm (6.424 eV) has been the subject of several investigations. Recently, the value of the branching ratio of 1.66 ± 0.3 for S(^3P)/S(^1D) was published [19]. The present work yields a similar value of 2.8 ± 0.4 (c.f. ref [30]), as will be discussed further below.

Additionally, a photolytical source of S(^{3}P) is needed in order to separate photoionization features of S(^{3}P) from those of S(^{1}D). Disulfur monoxide (S_2O) is chosen as a reference system. Photoabsorption and photodissociation of S_2O have been investigated in the past [31–34]. In the near ultraviolet (280-350 nm) a band system is observed that predissociates into S(^{3}P) and SO. Photolysis of S_2O within this band system is a source of atomic sulfur in only one well-defined quantum state, i.e. ^3P. Radiation from a XeCl excimer laser ($\lambda = 308$ nm(4.025 eV)) can be used to photolyze the precursor (see Section II).

On the theoretical side, photoionization cross sections calculations of the sulfur atom have previously been made by Conneely *et al.* [35] using the close-coupling approximation. These authors reported the parameters for the resonance series in the photoionization of sulfur from the ground state. Mendoza and Zeippen [36] using the R-matrix method (in the LS coupling scheme) calculated the photoionization cross sections of the ground states of Si, P, and S. Tayal [37] using the R-matrix method (in the LS coupling scheme) calculated the total and partial cross sections for the photoionization of the $3s^2 3p^4\ ^3P$ ground state of the sulfur atom for photon energies from the first $S^+(3s^2 3p^3\ ^4S^\circ)$ ionization threshold to about 25 eV. Photoabsorption cross sections of the ground state of four oxygen-group atoms were calculated using the eigenchannel R-matrix method by Chen and Robicheaux [38] within an LS - jj frame transformation to approximately include spin-orbit coupling effects. Tondello's [14] assignment of the $3s^2 3p^3(^2D^\circ)ns\ ^3D^\circ$ and $3s^2 3p^3(^2D^\circ)nd\ ^3S^\circ$ series was reversed by Gibson *et al.* [16] based on their considerations of the quantum defects of the two series. Tayal [37] suggested that these two series should not be reversed and agreed with the assignment of Tondello [14]. Mendoza and Zeippen [36] and Altun [39] did not give a conclusion about this disagreement. However, the calculations of Chen and Robicheaux [38] strongly confirmed that the assignment made by Tondello [14] was the correct one.

The layout of this paper is as follows. In Section II we give a brief overview of the experimental procedure. In Section III we outline the theoretical methods employed in our work. Section IV presents our experimental and theoretical results. The experimental setup was used to determine the photoionization cross section of atomic sulfur [S($3s^2 3p^4\ ^3P$) and S($3s^2 3p^4\ ^1D$)] in a broad energy range. Section V gives a brief discussion of them. Finally in Section VI we give a summary of our findings.

II. EXPERIMENT

Single-photon-ionization in combination with time-of-flight mass spectrometry is used to measure state-selectively the photoion yields of atomic sulfur species in the gas phase. The experimental setup has been described in detail elsewhere [40]. Briefly, the experimental setup consists essentially of the following components:

1. A tunable, pulsed VUV light source based on a laser-produced plasma [41]. The plasma is generated by focusing a Nd:YAG-Laser (Spectron Laser Systems, SL 400; 1064 nm, 500 mJ/pulse, 10 Hz, 6 ns pulse length) onto a tungsten wire target. A glass capillary is used to transfer the plasma radiation on the entrance slit of a normal incidence monochromator (McPherson, Model Nova 225). Plasma radiation is dispersed by a gold coated spherical reflection grating (1200 lines/mm). The absolute number of VUV photons is estimated to be of the order of 10^8 photons per pulse, corresponding to 10^9 photons per second at 10 Hz operation of the lasers, which is similar to previous work [24, 25, 42–44]. The typical bandwidth of the dispersed VUV photons is set to $\Delta\lambda \approx 2.4$ - 5.9 $\mathring{A}$, depending on the spectral features to be resolved in the respective energy regime. Calibration of the VUV source and its photon energy scale is performed by taking ion yields of molecular oxygen [40, 45]. The well-known vibrationally resolved transitions in the energy range between 12.19 and 13.78 eV are used for this purpose [46].

2. Pulsed ultraviolet lasers are used to photolyze precursor molecules. An ArF excimer laser (Lambda Physics, OptexPro, $\lambda = 193$ nm, 10 mJ/pulse, 10 Hz, 10 ns pulse length) serves to photolyze CS_2. The pulse energy is reduced to approximately 50 μJ due to the occurrence of strong multi-photon ionization signals from the photolysis laser. S_2O photoexcitation is carried out by a XeCl Laser (Lambda Physik LPX 202i; 200 mJ/Pulse, 10 Hz, 10 ns pulse length). The laser radiation is not attenuated since multiphoton processes are not observed for S_2O.

   The photolysis laser is time-correlated with the VUV-system by an external pulse generator. The delay time between the 193 nm (6.424 eV) pulse and the VUV pulse in of the order of 100–400 ns.

3. A time-of-flight mass spectrometer is used to detect cations resulting from photoionization by tunable VUV-radiation. The mass spectrometer works according to the Wiley-McLaren energy- and space focusing conditions with a typical mass resolution of $m/\Delta m \approx 100$ [47, 48]. Typical pressures in the ionization region of the time-of-flight mass spectrometer are of the order of $5 \cdot 10^{-6}$ mbar.

CS_2 is used in commercial quality (Sigma Aldrich) without further purification. It is effusively introduced into the high vacuum chamber by a needle valve.

Disulfur monoxide (S_2O) is synthesized using the method of Schenk and Steudel [49–51]:

$SOCl_2 + Ag_2S \rightarrow S_2O + 2\,AgCl$.

S_2O is introduced into the ionization region in a mixture with rare gases, such as argon or helium, which is due to the synthesis procedure.

Pump-probe photoionization mass spectra are recorded at constant VUV-photon energy. Photoion yields of specific masses, such as $m/z = 32$ (sulfur) are obtained from selecting the corresponding time-of-flight signal in a set of mass spectra that are recorded as a function of the VUV-photon energy.

Ion yields are normalized with respect to the photon flux by using a photomultiplier that is coated by sodium salicylate as a quantum converter [52].

III. THEORY

The study of the photo-absorption spectrum of atomic sulfur is interesting due to the open-shell features of this atom and the role played by electron correlation effects. In order to gauge the quality of our theoretical work we performed large-scale close-coupling calculations and compared them to the present experimental measurements. We have used an extended large-scale close-coupling model in our calculations on this system compared to our previous preliminary Breit-Pauli calculations [30]. In the present theoretical work we include 512 levels of the residual S^+ ion in the close-coupling calculations and perform all the cross section calculations within the relativistic Dirac Coulomb R-matrix approximation.

A. Dirac-Coulomb R-matrix

Recently developed Dirac Atomic R-matrix Codes (DARC) for parallel computing architectures [53–58] were used to treat photon interactions with this neutral atomic system. This suite of collision codes has the capability to cater for hundreds of levels and thousands of scattering channels [57–59]. Metastable states are populated in the present sulfur atom experiments and require additional theoretical calculations. We note that our work is of prime interest to astrophysics as outlined in the Introduction. High quality photoionization cross section calculations have been made on several complex systems (Fe-peak elements and Mid-Z atoms) of prime interest to astrophysics and plasma applications, indicating suitable agreement with high resolution measurements made at leading synchrotron light sources [57, 58, 60–62].

To benchmark theoretical results with the experimental measurements, photoionization cross sections calculations on this sulfur atom were performed for both the

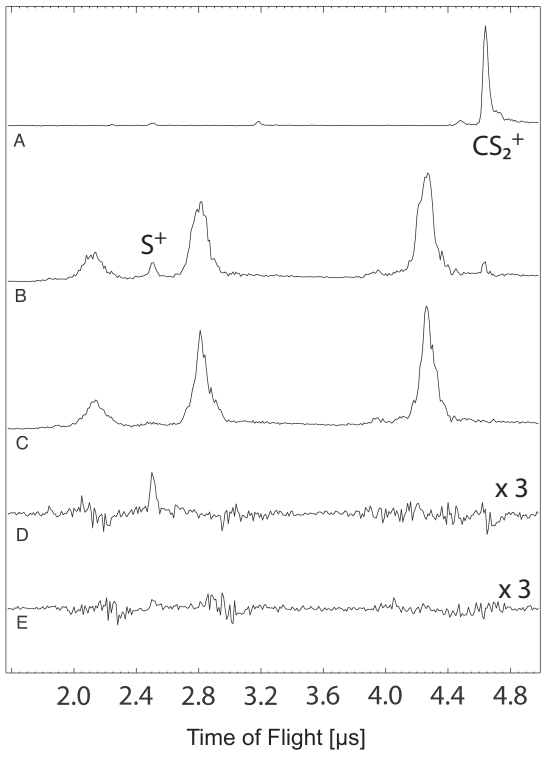

FIG. 1. Time-of-flight mass spectra of carbon disulfide (CS_2) recorded at different excitation conditions. (A) photoionization at λ=115.87 nm (10.70 eV); (B) primary photoexcitation 193 nm (6.424 eV) and subsequent photoionization (10.70 eV); (C) photoexcitation 193 nm (6.424 eV) without subsequent photoionization, indicating multi-photon ionization caused by 193 nm (6.424 eV) radiation; (D) difference (B)-(C); (E) similar to (D), but photoionization at 10.25 eV.

ground and the excited metastable levels associated with the $3s^23p^4$ configuration. Hibbert and co-workers have shown that two-electron promotions are important to include to get accurate energies, f-values and Einstein coefficients [63, 64] which are included in the present study. In our photoionization cross-section calculations for this element, all 512 levels arising from the eight configurations: $3s^23p^3$, $3s3p^4$, $3s^23p^23d$, $3s^23p3d^2$, $3s3p^33d$, $3p^33d^2$, $3p^5$, $3s3p^23d^2$ of the residual sulfur singly ionized ion were included in the close-coupling expansion. PI cross section calculations with this 512-level model were performed in the Dirac Coulomb approximation using the recently developed parallel version of the DARC codes [57, 58].

The R-matrix boundary radius of 13.28 Bohr radii was sufficient to envelop the radial extent of all the $n = 3$ atomic orbitals of the residual S^+ ion. A basis of 16 continuum orbitals was sufficient to span the incident experimental photon energy range from threshold up to 50 eV. This resulted in generating a maximum of 2,696 coupled channels in the close-coupling calculations with dipole and Hamiltonian matrices of the order of $\sim$ 32,525 in size. Similarly, here for the ground-state configuration, photoionization out of the $3s^23p^4\ ^3P_{2,1,0}$ levels require the bound-free dipole matrices, $J^\pi = 2, 1, 0^e \rightarrow J^\pi = 0^\circ, 1^\circ, 2^\circ, 3^\circ$ and for the excited $3s^23p^4\ ^1D_2$ and $3s^23p^4\ ^1S_0$ metastable states, the bound-free dipole matrices, $J^\pi = 0^e, 2^e \rightarrow J^\pi = 1^\circ, 2^\circ, 3^\circ$.

The current state-of-the-art parallel DARC codes running on high performance computers (HPC) world-wide, allows one to concurrently form and diagonalize large-scale Hamiltonian and dipole matrices [65, 66] required for electron or photon collisions with atomic systems. This allows large-scale computations to be completed in a timely manner.

B. Photoionization

In our calculations for the ground and metastable levels, the outer region electron-ion collision problem was solved with a fine mesh of 5×10^{-7} Rydbergs (≈ 6.8 μeV) to fully resolve the extremely narrow resonance features in the appropriate photoionization cross sections. The jj-coupled Hamiltonian diagonal matrices were adjusted so that the theoretical term energies matched the recommended experimental values of NIST [67]. We note that this energy adjustment ensures more reliable positioning of the resonances relative to all thresholds included in the calculations. Finally, in order to compare with experimental measurements, the theoretical cross-section calculations were convoluted with a Gaussian having a profile of width similar to the experiment resolution (44 meV FWHM).

C. Resonance structure

The energy levels tabulated from references [68, 69] and from the NIST tabulations [67] were used as a helpful guide for the present assignments.

The resonance series identification can be made from Rydberg's formula:

$$\epsilon_n = \epsilon_\infty - \frac{\mathcal{Z}^2}{\nu^2} \tag{1}$$

where in Rydbergs ϵ_n is the transition energy, ϵ_∞ is the ionization potential of the excited electron to the corresponding final state ($n = \infty$), i.e. the resonance series limit [70] and n being the principal quantum number. The relationship between the principal quantum number n, the effective quantum number ν and the quantum defect μ for an ion of effective charge $\mathcal{Z}$ is given by $\nu =$

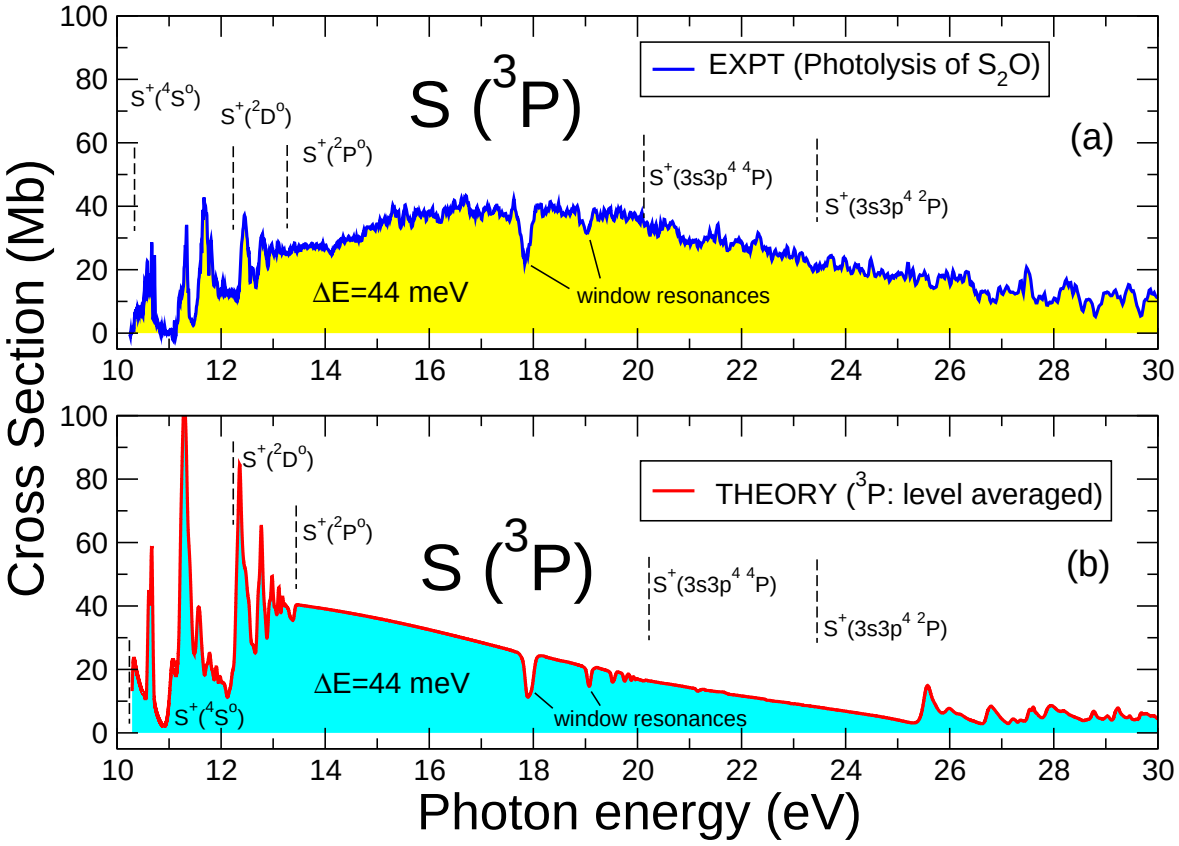

FIG. 2. (Color online) Photoionization of S($3s^2 3p^4\ ^3P$) in the energy range from threshold up to 30 eV. The various Rydberg series limits are illustrated, namely $S^+[3s^2 3p^3(^2D^\circ_{3/2,5/2})]$ and $S^+[3s^2 3p^3(^2P^\circ_{1/2,3/2})]$ by vertical dashed lines. The prominent window resonances are clearly visible. (a) The experimental cross section data are taken at a nominal energy resolution of 44 meV. (b) Theoretical cross sections for 100% of the S($3s^2 3p^4\ ^3P$) initial state from the 512-level DARC calculations (level averaged), convoluted with a Gaussian profile having a FWHM of 44 meV. The corresponding series limits E_∞ of Equation (2) for each series are indicated by vertical-dashed lines.

n $-\ \mu$. Converting all quantities to eV we can represent the Rydberg resonance series as;

$$E_n = E_\infty - \frac{\mathcal{Z}^2 \mathrm{R}}{(n-\mu)^2}. \qquad (2)$$

Here, E_n is the resonance energy, E_∞ the resonance series limit, $\mathcal{Z}$ is the charge of the core (in this case $\mathcal{Z} = 1$), μ is the quantum defect, being zero for a pure hydrogenic state, and the Rydberg constant R is 13.6057 eV.

The multi-channel R-matrix eigenphase derivative (QB) technique, which is applicable to atomic and molecular complexes, of Berrington and co-workers [71–73] was used to locate and determine the resonance positions in Tables II and III. The resonance width Γ is determined from the inverse of the energy derivative of the eigenphase sum δ at the resonance energy E_r via

$$\Gamma = 2\left[\frac{d\delta}{dE}\right]^{-1}_{E=E_r} = 2[\delta']^{-1}_{E=E_r} \quad . \qquad (3)$$

IV. RESULTS

A. Experimental Results

Fig. 1 shows time-of-flight mass spectra of carbon disulfide (CS_2) recorded at different excitation condi-

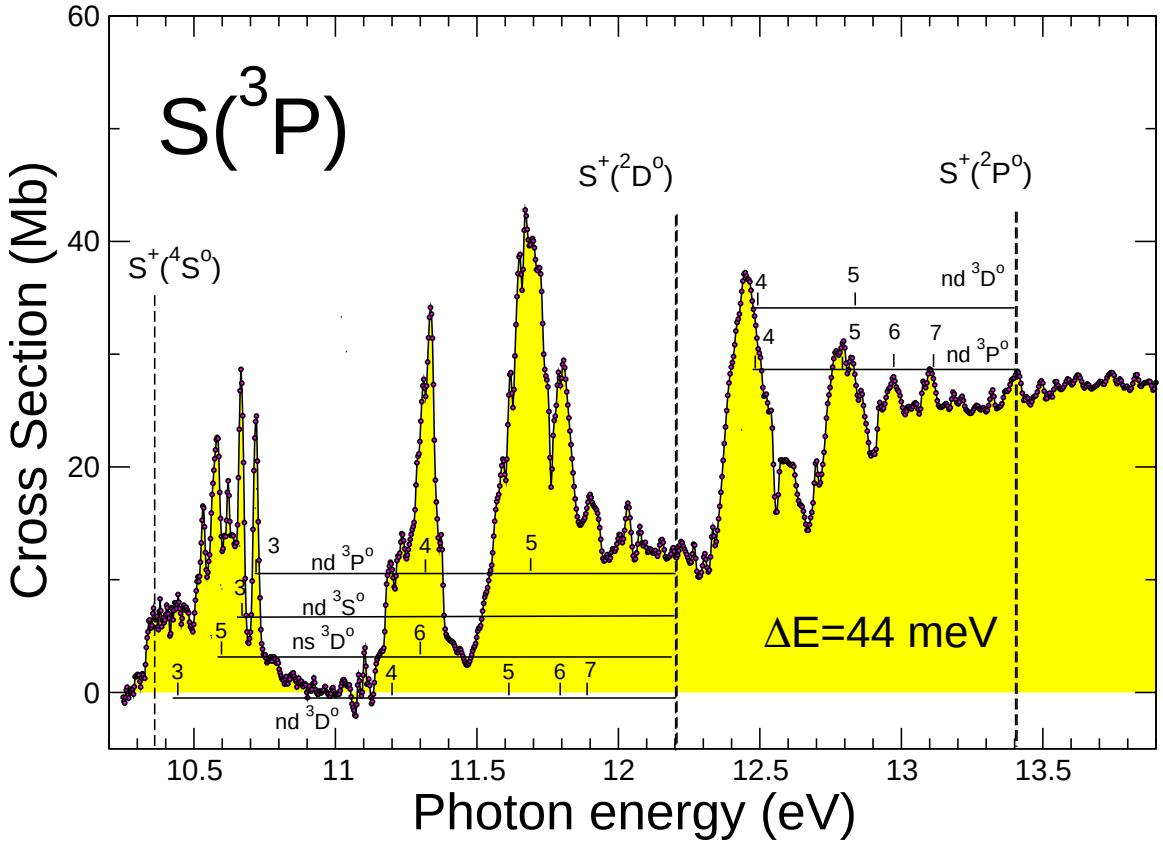

FIG. 3. (Color online) An overview of the present single photoionization cross-sections measurements as a function of the photon energy below 13.5 eV. The experimental measurements were made at a nominal energy resolution of 44 meV. The assigned Rydberg series limits are indicated as vertical lines grouped by horizontal lines. The corresponding series limits E_∞ of Equation 2 for each series are indicated by vertical-dashed lines in the end of the line groups. See text for a discussion of these resonance features.

tions. The top spectrum (Fig. 1(A)) shows the photoionization of CS_2 where 10.70 eV radiation is used. This photon energy is well above the photoionization threshold of 10.076 eV of CS_2 [74]. The parent cation CS_2^+ (m/z = 76) is observed at t=4.64 μs. Additional weak intensity above t=4.64 μs comes from isotopomers such as $C^{32}S^{34}S$. Weak signals occur at t=2.51 μs (m/z = 32) and at t=3.18 μs (m/z = 44). They are assigned to S^+ and CS^+ , respectively. These do not come from 10.70 eV photoionization of CS_2 since the threshold of ionic fragmentation of CS_2 is 14.80 eV [74]. Rather, these ions are due to dissociative photoionization of CS_2 that is caused by second-order radiation from the monochromator (E= 21.4 eV, see Section II.). A weak signal at t = 4.48 μs is attributed to impurities in the sample.

Fig. 1(B) shows the mass spectrum for primary photolysis of CS_2 (193 nm (6.424 eV)) with subsequent (Δt=400 ns) photoionization at 10.70 eV. This spectrum is drawn on the same scale as Fig. 1 (A). The CS_2^+-signal is much weaker, whereas additional broad signals are observed around 2.1 μs, 2.8 μs, and 4.25 μs, respectively. These are due to dissociative multiphoton ionization of CS_2. They are time-shifted by $\approx$ 0.4 μs, which is the delay time between the 193-nm photolysis and subsequent photoionization by a 10.70 eV photon pulse. This delay facilitates the assignment of signals that come from multiphoton ionization. The width of these signals is due to (i) a jitter in the delay time between the laser pulses and (ii) a kinetic energy release during the multiphoton ionization process that is not discussed further.

The main feature of mass spectrum (B) regarding the formation of atomic sulfur by photolysis is an enhanced

intensity of the S^+ signal at t =2.51 μs. This is apparently *not* due to multiphoton ionization since the signal is absent if *exclusively* 193-nm radiation is used (cf. Fig. 1 (C)).

The difference between the spectra 1 (C) and (B) is shown in Fig. 1 (D). The only signal that remains after the subtraction is S^+. It implies that the S^+ signal comes from a two-step process:
(i) photolysis of neutral CS_2 (193 nm (6.424 eV) radiation), leading to the formation of atomic sulfur according to
$CS_2 \xrightarrow{193\ \text{nm}} S + CS$
(ii) photoionization of atomic sulfur generated in step (i):
$S \xrightarrow{10.70\ \text{eV}} S^+$.

The ionization energy of atomic sulfur in its ground state $S(^3P_2)$, leading to $S^+\left(^4S^0_{3/2}\right)$ is 10.36001 eV [75], so that S^+ from photoionization of $S(^3P_2)$ is a source of S^+. Electronically excited $S(^1D_2)$ has an excitation energy of 1.145 eV [75] so that the ionization energy of this state is reduced to 9.215 eV. Photoionization of the $S(^1D)$ state into the ^4S continuum is possible from an energetic point of view; however, $S(^1D)$ can only be autoionized at this photon energy, since direct photoionization into the $^4S^o$ ground state of S^+ is spin-forbidden.

The S^+ signal may therefore contain contributions from both $S(^3P)$ and $S(^1D)$. Selecting this signal and recording its intensity as a function of the VUV energy leads to the S^+ ion yield of photolyzed CS_2 which may come from both quantum states produced in CS_2 photolysis, i.e. $S(^3P)$ and $S(^1D)$. There are two difficulties connected with the S^+ ion yield from 193 nm (6.424 eV) photolysis of CS_2:

(i) Atomic sulfur is produced in a mixture of it lowest-lying ^3P and ^1D states, as outlined in Section I. In order to separate the ^1D yield from the ^3P yield, S_2O is used as a reference system, which exclusively yields $S(^3P)$ upon photolysis.

The experimental procedure is similar to that described above for CS_2. Photolysis and subsequent photoionization yields S^+. By recording the S^+ intensity as a function of VUV photon energy we obtain the yield for photoionization and autoionization of pure $S(^3P)$.

The S^+ ion yield from S_2O is scaled with respect to the S^+ yield from CS_2 so that the relative intensities of resonant features that come from photoioization of $S(^3P)$ have the same intensity in both spectra. The S^+ yield originating from S_2O is subsequently subtracted from the S^+ yield which is obtained from CS_2. This provides the ionization yield of pure $S(^1D)$, provided that other sources of S^+ are of negligible importance.

(ii) We note that there are indeed additional channels at higher VUV photon energy leading to the formation of S^+, so that the S^+ yield may have other origins than $S(^1D)$. These are listed in Table I, where channels (3) and (4) from CS_2 as well as (6) and (7) from S_2O need to be considered.

As a result, additional subtraction processes have to be carried out in order to remove such additional S^+ intensity, originating from other sources besides $S(^1D)$, as indicated in Table I. Specifically, the S^+ yield that is attributed to ionization of $S(^1D)$ likely contain contributions from such channels, as will also be outlined in the following in comparison with the modeling results.

B. Cross-Sections

The electronic ground state of atomic sulfur is $(3s^2 3p^4\ ^3P)$ having the electron configuration $3s^2 3p^4$ and by spin-orbit effects splits into the three fine-structure states namely, $3s^2 3p^4\ ^3P_{2,1,0}$. The difference in energy between the ground state $3s^2 3p^4\ ^3P_2$, $3s^2 3p^4\ ^3P_1$, and the $3s^2 3p^4\ ^3P_0$ states is 49 and 71 meV [67], respectively. Note, at room temperature the sulfur atom is primarily in the $3s^2 3p^4\ ^3P_2$ state, which is why contributions from the other two states may be neglected. Similarly, the electronic configuration of the positively charged sulfur ion (S^+) in the $3s^2 3p^3$ configuration can form the states $^4S^o$, $^2D^o$, and $^2P^o$. The continuum states are energetically located at 10.36 eV, 12.20 eV, and 13.40 eV above the electronic ground state of the neutral atom [67]. The states formed are analogous to isoelectronic atomic oxygen, taking into account the emitted photoelectron terms that are relevant to the optical transitions. The uni-positive $^4S^o$ state with spin $S = 3/2$, together with the electron spin $s = \pm\ 1/2$ gives a total spin of 1 or 2, hence triplet and quintet terms may arise. An analogous procedure results for the case of the $^2D^o$ and $^2P^o$ excited states, where both singlet and triplet terms are formed. Optical excitation from the ground state of the $3s^2 3p^4\ ^3P_2$ sulfur atom in the sense of the spin selection rule $\Delta\ S = 0$ then makes all three continuum states allowed.

Few experimental measurements have been performed for the absolute photoionization cross section of the ground state of atomic sulfur. As pointed out in the Introduction, Tondello [14] measured the absorption spectrum of atomic sulfur giving the first values for the ionization cross section. Absolute photoionization cross sections at a photon energy of 14.76 eV were published by Innocenti et al. [77] who found a cross section value of 75 Mb. Extrapolation of these results to a photon energy of 16.7 eV, gave a value of 68.7 Mb having a 50% absolute error and larger than the 50 Mb estimated from the absolute measurements of Joshi and co-workers [17] which are estimated to have a 25% error. This photon energy was chosen as theoretical work is available from the Hartree-Fock-Slater method by Yeh and Lindau [78] which gave a cross-section value of 18.2 Mb. The accuracy of the measurements carried out by Tondello [14] are 50% higher than these very approximate calculations. In the present work the absolute photoionization cross section for $S(^3P)$ at a photon energy of 16.7 eV yields a value of 43.5 $\pm$ 10 Mb. Preliminary calculations using the Breit-Pauli ap-

TABLE I. Threshold energy (TE) in eV of S^+ from CS_2 and S_2O precursors. The product channels are sorted by increasing threshold energy (eV) for each precursor. Secondary photodissociation products of primary photofragments, such as S from CS or SO photodissociation with subsequent photoionization are considered to be of minor intensity, so that they are not listed. Calculated threshold energies (eV) are based on data taken from Ref. [76]. Transition probabilities and selection rules are not taken into account.

Source	$\frac{\text{TE}}{(\text{eV})}$	Pathway to S^+	
CS_2	9.21	$CS_2 \xrightarrow{\text{photolysis}} S(^1D)+CS \xrightarrow{VUV} S^+ + CS$	(1)
CS_2	10.36	$CS_2 \xrightarrow{\text{photolysis}} S(^3P)+CS \xrightarrow{VUV} S^+ + CS$	(2)
CS_2	14.80	$CS_2 \xrightarrow{\text{VUV}} CS + S^+$	(3)
CS_2	18.21	$CS_2 \xrightarrow{\text{photolysis}} S(^3P,\ ^1D)+CS \xrightarrow{VUV} S + CS^+ \xrightarrow[\text{fragm.}]{\text{ionic}} S + C + S^+$	(4)
S_2O	10.36	$S_2O \xrightarrow{\text{photolysis}} S(^3P)+SO \xrightarrow{VUV} S^+ + SO$	(5)
S_2O	13.76	$S_2O \xrightarrow{\text{VUV}} SO + S^+$	(6)
S_2O	15.72	$S_2O \xrightarrow{\text{photolysis}} S(^3P)+SO \xrightarrow{VUV} S + SO^+ \xrightarrow[\text{fragm.}]{\text{ionic}} S + S^+ + O$	(7)

Notes: (1-2, 5): taken from Ref. [75]; (3): cf. Ref. [74]; (4, 7): calculated by using the dissociation energy of CS and SO according to Ref. [76] and the ionization energy of $S(^3P)$ according to Ref. [75]; (6): taken from Ref. [30].

proximation (in the framework of the *R*-matrix method at this photon energy) produces a value of 42.8 Mb [30]. The present level averaged DARC calculations produces a value of 33 Mb. These theoretical values are in accord with both the *R*-matrix *LS*-coupling results of Tayal [37] and the many-bodied perturbation estimates carried our by Altun [39]. The present photoionization cross-section calculations are greatly extended within the confines of the Dirac *R*-matrix method. We investigated the photon energy region from thresholds up to 30 eV. All the resonance structure converging to the $S^+(^2D^o_{3/2,5/2})$ and $S^+(^2P^o_{1/2,3/2})$ thresholds and the associated window resonances converging to the $S^+(3s3p^4\ ^{2,4}P_J)$ ionic thresholds is analyzed and discussed.

C. Photoionization of S$(3s^23p^4\ ^3P)$

Photoionization of the ground state of atomic sulfur $S(3s^23p^4\ ^3P)$ was examined using the photodissociation of S_2O, which is initiated by photolysis with 308 nm (4.025 eV) radiation, yielding $S(^3P)$. Detection is accomplished by one-photon ionization using VUV radiation from a laser produced plasma. Using the observed autoionization resonances in the photon energy range below 13.40 eV and the window resonances converging to the ^4P threshold at 20.20 eV, allows us to identify $S(3s^23p^4\ ^3P)$ as the sole photolysis product from S_2O. The experimental technique of the present work is a valuable alternative to that used by other authors who used H_2S with hydrogen and fluorine radicals in a flow system [16, 79].

An overview of the experimental photoionization spectrum from the $S(3s^23p^4\ ^3P)$ ground state taken at an energy resolution of ΔE=44 meV is show in Figure 2 (a) and the results from the DARC calculations are illustrated in Figure 2 (b). The theoretical cross sections were convoluted with a Gaussian having a width of 44 meV in order to simulate the experimental results. We note that strong resonance features are observed in the cross section below 13 eV and there is a prominent window resonance located at approximately 18 eV. Figure 3 illustrates the experimental cross section for the $S(3s^23p^4\ ^3P)$ ground state in the photon energy region from threshold to approximately 13.9 eV. The intensity of the resonant structures in the cross sections below 12 eV in comparison with the continuous region 14 – 17 eV appear to be more prominent in the theoretical spectrum than in the experimental results, due to the limited energy resolution available in the experimental results. In addition to the direct photoionization, there are a number of partial auto-ionizing Rydberg series that are optically allowed. We note, from the $S(3s^23p^4\ ^3P)$ ground state of atomic sulfur, excitation into the ns and nd Rydberg states are possible giving the $3s^23p^3(^2D^o)n\ell\ ^3L^o$ and $3s^23p^3(^2P^o)n\ell\ ^3L^o$ Rydberg resonance series, where ℓ is s or d. In the case of the $^2D^o$ kernel, four Rydberg series are possible: $^3D^o$ from the ns-Rydberg orbitals and $^3S^o$, $^3P^o$, and $^3D^o$ from the nd Rydberg orbitals. For the $^2P^o$ core there are three optically allowed series; $^3P^o$ from the ns-Rydberg orbitals and $^3P^o$, $^3D^o$ from the nd-Rydberg orbitals.

D. Rydberg resonance series of S$(3s^23p^4\ ^3P)$

As illustrated in Figure 3, the first ionic continuum $^4S^o$ manifests itself in the cross section for $S(3s^23p^4\ ^3P)$, as obtained from the photolysis of S_2O. There is a sud-

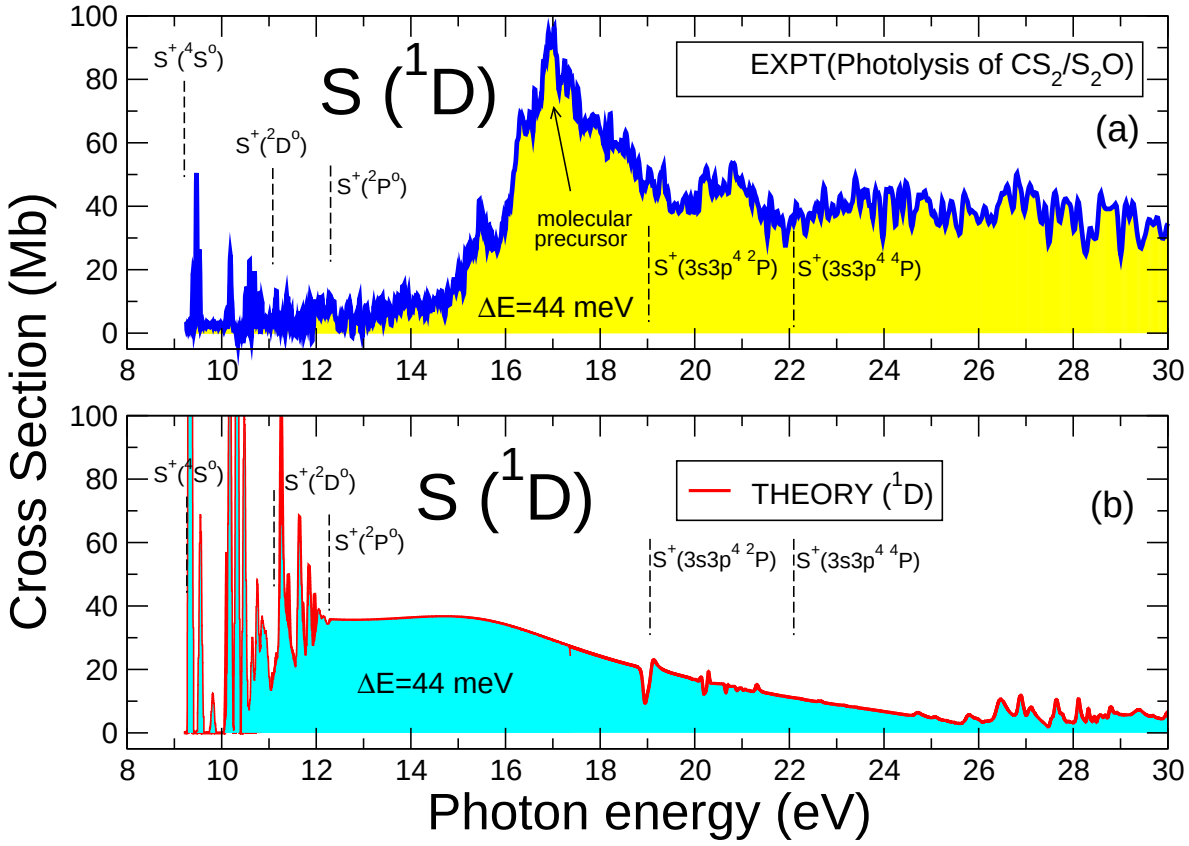

FIG. 4. (Color online) An overview of the experimental measurements on S(^1D) as a function of the photon energy; (a) experiment for the S($3s^2 3p^4\ ^1D$) metastable state over the energy range from threshold to 30 eV. Primary photolysis of CS_2 was carried out at λ =193 nm (6.424 eV). Contributions from ionic fragmentation photolysis of CS_2 are not subtracted. The curve is normalized to the VUV-photon flux. (b) Theoretical cross section results for 100% of the S($3s^2 3p^4\ ^1D$) metastable state from the DARC calculations convoluted at 44 meV. The resonance series limits E_∞ of Equation (2) for each series are indicated by vertical-dashed lines in the end of the line groups. Resonance features from this Figure are tabulated in Table II.

den increase in ion yield at a photon energy of 10.35 ± 0.02 eV, although there is a relatively weak continuum. This is particularly evident in the decrease in the photoionization cross section value around 11 eV similarly observed by Gibson and co-workers [16]. The $S^+(^2D^o)$ and $S^+(^2P^o)$ ionic thresholds (respectively at 12.20 eV and 13.40 eV), are partially overlaid with autoionizing Rydberg states. In the present work, detailed measurements were made up to the photon energy of 13.40 eV, for the case of resonance series converging to the $S^+(^2P^o)$ threshold from the initial S($3s^2 3p^4\ ^3P$) state. For the S($3s^2 3p^4\ ^3P$) state, shown in Figure 3, strong resonance series are observed in the photon energy range 12.20 - 13.4 eV, i.e. below the $S^+(^2P^o)$ threshold. The assignments and positions of these Rydberg resonance series are in suitable agreement with the NIST tabulations [67].

It is expected that all members of $3s^3 3p^3(^2P^o)n\ell$ Rydberg resonance series (with the exception of the $3s^3 3p^3(^2P^o)ns\ ^3P^o$ series), converging to the $S^+(^2P^o)$ threshold are observed. Members of this group were seen in the early work of Gibson and co-workers [16] as shoulders of the $3s^3 3p^3 nd\ ^3P^o$ series but are not observed in the present work which is primarily due to the limited energy resolution of the tunable VUV plasma source. Individual members of the various $3s^2 3p^3(^2D^o)n\ell$ series; $nd\ ^3D^o$, $ns\ ^3D^o$, $nd\ ^3S^o$ and $nd\ ^3P^o$ series can be identified. At photon energies of 10.557 eV, 10.561 eV, and 10.646 eV we find the triplet Rydberg states $3s^2 3p^3(^2D^o)3d\ ^3P^o$, $3s^2 3p^3(^2D^o)5d\ ^3P^o$, and $3s^2 3p^3(^2D^o)6d\ ^3P^o$. However, due to the narrow line

width of the resonances and the limited energy resolution (44 meV FWHM), many of the resonances were not resolved. A similar situation occurred for the resonances associated with the $3s^3 3p^3(^2P^o)nd\ ^3P^o$ and the $3s^3 3p^3(^2P^o)nd\ ^3D^o$ Rydberg resonance series.

E. Window resonances of S($3s^2 3p^4\ ^3P$)

In atomic sulfur, the $3s3p^4\ ^4P$ and $3s3p^4\ ^2P$ ionization states (occurring from a 3s vacancy state) are located at 19.056 eV and 22.105 eV, respectively. In the observed photoionization spectra of atomic sulfur for the ($3s^2 3p^4\ ^3P$) ground state (in the photon energy range 17.8 – 20.2 eV) we observe two prominent members of a Rydberg series of window resonances. These features were also seen in the early theoretical work of Altun and co-workers [39]. These dip-like structures were first observed in this photon region by Innocenti and co-workers [77] using constant ionic state (CIS) spectroscopy. Innocenti and co-workers [77] showed that these window resonance originate from the $3s^2 3p^4$ parent configuration and are due to the $3s \rightarrow np$ excitation being members of the $3s3p^4np$ Rydberg resonance series.

The ground state electronic configuration of the sulfur atom is ($3s^2 3p^4\ ^3P$), i.e. valence shell photoionization from this state produces the ionic continuum states $S^+(^4S^o)$, $S^+(^2D^o)$ and $S^+(^2P^o)$, which have ionization potentials of 10.36 eV, 12.20 eV, and 13.40 eV [67]. Inner-shell 3s ionization results in the S^+ ionic $3s3p^4\ ^4P$ and $3s3p^4\ ^2P$ hole states that have ionization potentials of 20.20 eV and 23.45 eV, respectively [67, 77]. The window resonances occur due to excitation first into a Rydberg resonance state caused by autoionization, then into the energetically accessible $^4S^o$, $^2D^o$, and $^2P^o$ continua transitions. The Rydberg states involved are triplet states, so the oscillator strengths for transitions violate the spin-selection rule $\Delta S = 0$, which in the case of atomic sulfur is very low. The most intense transitions occur for ΔL = 0, ± 1, in this case $ns \rightarrow np$ transitions are expected to occur.

The dipole selection rule (ΔL = 0, ± 1) limit the allowed Rydberg resonance states to the $3s3p^4(^4P)np\ ^3D^o$, $3s3p^4(^4P)np\ ^3P^o$ and $3s3p^4(^4P)np\ ^3S^o$ resonance series, where the assignments are based on earlier work of Innocenti et al. [77]. Their experimental work has already revealed the position of members of these resonance series. In the present study the first two members of the resonance series were observed at 17.82 ± 0.09 eV (69.57 ± 0.35 nm) and 19.02 ± 0.09 eV (65.19 ± 12.35 nm), respectively, which is in good agreement with the experimental work of Innocenti et al. [77]. Our present theoretical estimates are also in respectable agreement with the present experimental work. The resonances are very intense and couple to the $^2D^o$ and $^2P^o$ continuum. Other members of this Rydberg resonance series are obtained at 19.55 ± 0.09 eV and 19.78 ± 0.09 eV which agree well with the results of Innocenti et al. [77]. Innocenti and co-workers [77] observed that both of the n=3 and 4 members of this Rydberg resonance series have a spectral line-width just below the experimental resolution. In the present work, the window resonances are observed by detection of the S^+ ions from photoionization of atomic sulfur in the S($3s^2 3p^4\ ^3P$) ground state.

Similar types of structures were observed previously by Angel and Samson [80] for atomic oxygen. Window resonances were also observed for atomic selenium, by Gibson et al. [16] and atomic tellurium, by Berkowitz et al. [81]. However, in all these previous studies, the structures are clearly less intense than in the present case of atomic sulfur.

F. Photoionization of metastable S($3s^2 3p^4\ ^1D$ and ^1S)

The photoion yield of atomic sulfur in the S($3s^2 3p^4\ ^3P$) state, using CS_2 as a precursor, allows us to obtain photoion yield curves of atomic sulfur, in the S ($3s^2 3p^4\ ^3P$) and S($3s^2 3p^4\ ^1D$) states. By subtraction means, the excited metastable state of atomic sulfur S ($3s^2 3p^4\ ^1D$) is then accessible. The excited S($3s^2 3p^4\ ^1D$) metastable state of atomic sulfur is of fundamental spectroscopic interest because here the behavior of electronically excited states of systems can be analyzed. The S($3s^2 3p^4\ ^1D$) metastable state of atomic sulfur is located at 1.145 eV above the S($3s^2 3p^4\ ^3P$) ground electronic state, where the first three ionization energies (for the $^4S^o$, $^2D^o$ or $^2P^o$ continuum) are located at 9.215 eV, 11.060 eV, and 12.25 5 eV, respectively.

Previous experimental studies on the photoionization of atomic sulfur in the first electronically excited metastable state S($3s^2 3p^4\ ^1D$) are rather limited in energy range. The work of Pan and co-workers [23] studied the energy 75 800 – 89 500 cm^{-1} (9.4 - 11.1 eV), using dissociation of CS_2 after photolysis at 193 nm (6.424 eV) produced sulfur atoms in a singlet excited states which were subsequently ionized by synchrotron radiation. A resolution of up to 3 cm^{-1} (0.37 meV) was attainable at the NSRRC beamline U9CGM in China. Several Rydberg resonances series were detected and analyzed converging to the $S^+(^2D^o_{3/2,5/2})$ thresholds.

On the theoretical side several studies of atomic sulfur dealing with the transitions and energies of the ground $3s^2 3p^4\ ^3P_2$ and metastable $3s^2 3p^4\ ^1D_2$ states are available in the literature as mentioned in the Introduction. Experiments were first performed by Joshi and co-workers [17] for the case of the sulfur atom in the $3s^2 3p^4\ ^1D_2$ state for the energy range below the $S^+(^2P^o)$ threshold, which is located at 12.255 eV. Two Rydberg series were detected in the gas phase absorption spectrum. The photon energy range studied in previous experiments carried out below the $S^+(^2D^o)$ threshold (located at 11.060 eV) is rather limited. The work of Qi et al. [82] investigated photoionization of atomic sulfur in the initial S($3s^2 3p^4\ ^1D$) state, from the 193 nm (6.424

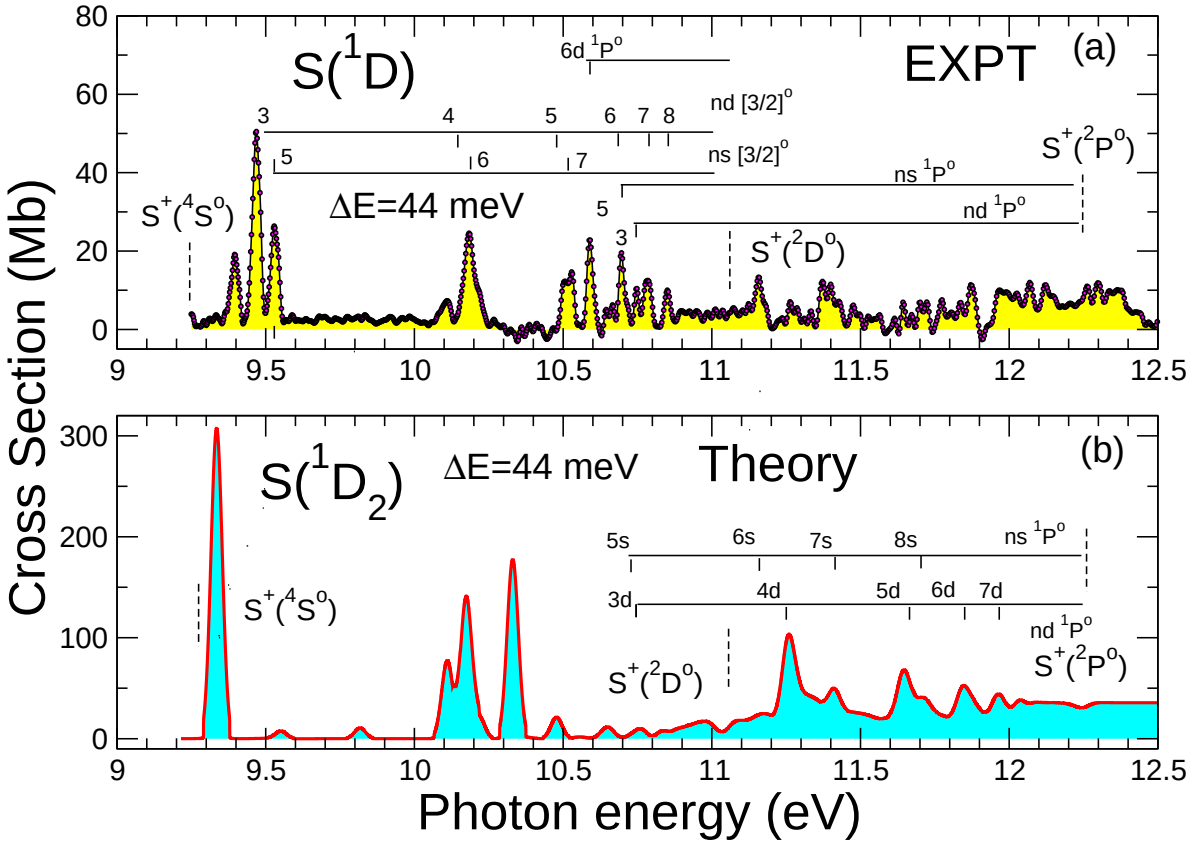

FIG. 5. (Color online) Single photon ionization of sulfur as a function of the photon energy. (a) The experimental cross section is recorded with a nominal energy resolution of 44 meV. The assigned Rydberg series are indicated by vertical lines grouped by horizontal or inclined lines. The corresponding series limits E_∞ of Equation 2 for each series are indicated by vertical-dashed lines at the end of the line groups. The first few values of n for each series is displayed close to its corresponding vertical line in each group. (b) Single photoionization of atomic sulfur as a function of the photon energy in the $3s^2 3p^4\ ^1D$ metastable state from threshold to 12.5 eV. Theoretical cross section were carried out with the DARC codes, and convoluted with a Gaussian having a profile of 44 meV. The assigned Rydberg series are indicated as vertical lines grouped by horizontal or inclined lines. The corresponding series limits E_∞ of Equation 2 for each series are indicated by a vertical-dashed lines in the end of the line groups. Resonance energies and quantum defects for the series lying below the $S^+(^2D^o_{3/2,5/2})$ thresholds are tabulated in Table II.

eV) excitation of thiethane (C_3H_6S) up to a photon energy of 13.5 eV using synchrotron radiation at 200 meV FWHM resolution. However, the energies of their observed Rydberg resonances series neither agree with the findings of other authors nor with the present work.

In the photon energy region below 11.060 eV, the use of the $^2D^o$ continuum relative to the energy of $S(3s^2 3p^4\ ^1D)$, has been studied by a variety of different authors where the known autoionizing Rydberg resonances series were resolved. Experiments were primarily carried out by tunable VUV radiation employing frequency tripling of UV laser radiation. The high resolving power permitted to determine the lifetimes of some of the excited Rydberg states. A disadvantage of this approach though is the very limited frequency (energy) range investigated, as it excludes photoionization studies at higher photon energies and broad tuning of the radiation.

In the present work, by appropriate subtraction of the photo-ion yield curve, from the photolysis process of CS_2, both states of the sulfur species, $S(3s^2 3p^4\ ^3P)$ and $S(3s^2 3p^4\ ^1D)$ can be studied. The photo-ion yield curve of atomic singlet sulfur $S(3s^2 3p^4\ ^1D)$ was determined in

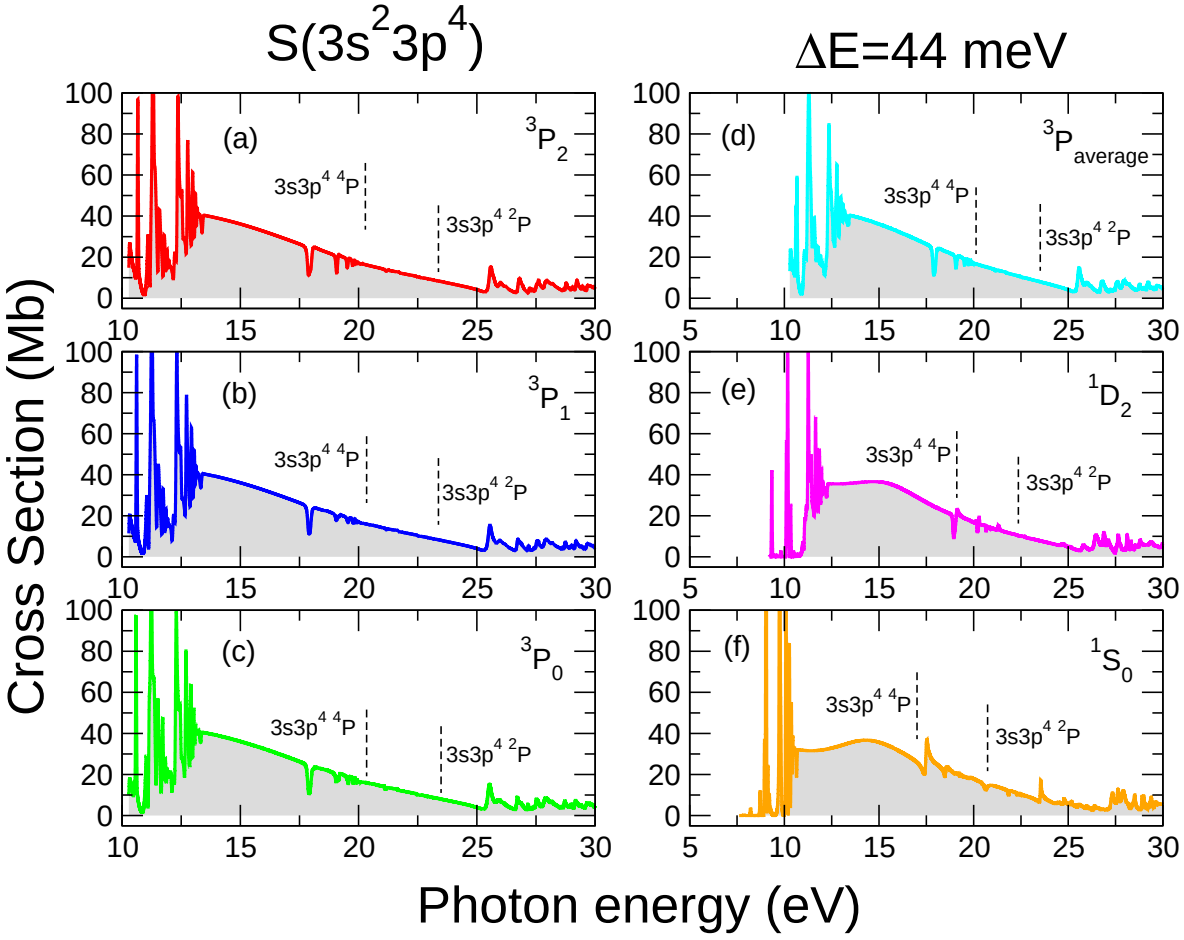

FIG. 6. (Color online) Theoretical cross sections from the 512 level DARC calculations for sulfur $3s^2 3p^4\ ^3P_{2,1,0}$, and $3s^2 3p^4\ ^1D_2$, and $3s^2 3p^4\ ^1S_0$ initial states convoluted with a Gaussian profile of 44 meV. Single photoionization cross sections of the sulfur atom as a function of energy over the photon energy from thresholds to 30 eV illustrating strong resonance features in the spectra below 14 eV. (a) $3s^2 3p^4\ ^3P_2$, (b) $3s^2 3p^4\ ^3P_1$ (c) $3s^2 3p^4\ ^3P_0$, (d) $3s^2 3p^4\ ^3P$ level averaged, (e) metastable $3s^2 3p^4\ ^1D_2$ and (f) metastable $3s^2 3p^4\ ^1S_0$ cross sections. The corresponding series limits E_∞ of Equation 2 for the window resonances converging to $3s3p^4\ ^4P$ and $3s3p^4\ ^2P$ sulfur ion thresholds are indicated by vertical-dashed lines.

the photon energy range up to 30 eV. The analysis of the relative intensities of the autoionization resonances, originating from S($3s^2 3p^4\ ^1D$) and S($3s^2 3p^4\ ^3P$) states that are formed by photolysis of CS_2, aids to determine both sulfur states ($3s^2 3p^4\ ^3P$ and $3s^2 3p^4\ ^1D$). From our experimental studies, Rydberg resonances associated with the S($3s^2 3p^4\ ^1D$) initial atomic state are found to be located at 9.47 ± 0.02 eV and at 10.21 ± 0.02 eV, respectively. Similarly for the $S(3s^2 3p^4\ ^3P)$ state, resonances are found located at 10.72 ± 0.02 eV, 11.34 ± 0.07 eV and 11.66 ± 0.07 eV. The relatively high margin of error arises from the uncertainty in the scaling of the absolute photoionization cross-section to the theoretically calculated values.

The branching ratio of these atomic sulfur species formed by photolysis can be reliably determined. Under the present experimental conditions we find the branching ratio S(^1D_J)/S(^3P_J) = 2.8 ± 0.4 at a photolysis wavelength of 193 nm (6.424 eV). The ratio of 2.8 ± 0.4 found in favor of of S($3s^2 3p^4\ ^1D$) is in clear contradiction to earlier work, where S($3s^2 3p^4\ ^3P$) is the more abundant species. Waller et al. reported a branching ratio S(^3P_J)/S(^1S_J) = 2.8 ± 0.3 [83] and 1.6 ± 0.3 was reported by Xu et al. [19], also in favor of S(^3P). However, the present value of 2.8 ± 0.4 in favor of the S($3s^2 3p^4\ ^1D$) state agrees with that found by Yang et al [21, 22]. There is no plausible explanation for the large discrepancy in the experimental values for the branching ratio of S($3s^2 3p^4\ ^1D$) to S($3s^2 3p^4\ ^3P$) from the 193 nm (6.424 eV) photolysis of CS_2. It is assumed that likely

TABLE II. Principal quantum numbers n, resonance energies (eV), and quantum defects μ of the prominent $S(3s^2 3p^3[^2D^\circ_{5/2,3/2}])ns, nd$ Rydberg series seen in the $S(3s^2 3p^4\ ^1D_2)$ photoionization spectra converging to the $S^+(3s^2 3p^3[^2D^\circ_{3/2,5/2}])$ and $S^+(3s^2 3p^3[^2P^\circ])$ thresholds. The experimental resonance energies are calibrated to ±20 meV and quantum defects μ are estimated to within an error of 20%. The assignments are shown in Fig. 5. The theoretical results are obtained from the 512-level DARC calculations performed within the Dirac Coulomb R-matrix approximation. The experimental spectral assignments, from the thesis work of Barthel [30], are uncertain for entries in parentheses.

Sulfur (Initial state)		E_n (eV) (Expt)	E_n (eV) (Theory)	μ (Expt)	μ (Theory)	E_n (eV) (Expt)	E_n (eV) (Theory)	μ (Expt)	μ (Theory)
	ns		$3s^2 3p^3(^2D^\circ_{3/2})ns$	[3/2]			$3s^2 3p^3(^2D^\circ_{5/2})ns$	[5/2]	
$3s^2 3p^4\ ^1D_2$									
	5	(9.5300)[a]	9.5515	2.02 ± 0.40	1.99	–	–	–	
	6	(10.2046)[a]	10.2399	2.01 ± 0.40	1.93	–	10.2192		0.98
	7	(10.5136)[a]	10.5125	2.00 ± 0.40	2.01	–	10.5115		2.02
	8	–	10.6848	–	1.98	–	10.6785	–	2.03
	9	–	10.7840	–	1.98	–	10.7793	–	2.04
	10	–	10.8485	–	1.98	–	10.8442	–	2.07
	11	–	10.8929	–	1.97	–	10.8891	–	2.08
	...	...	...	–	...	...	...	...	...
	∞	11.0599[b]	11.0599[b]	–		11.0603[b]	11.0603[b]		
	nd		$3s^2 3p^3(^2D^\circ_{3/2})nd$	[3/2]			$3s^2 3p^3(^2D^\circ_{5/2})nd$	[5/2]	
$3s^2 3p^4\ ^1D_2$									
	3	(9.4690)[a]	9.4722	0.08 ± 0.02	0.07	–	–		
	4	(10.1715)[a]	10.1739	0.09 ± 0.02	0.08	(10.08762)[a]	10.1112	0.26 ± 0.05	0.21
	5	(10.4926)[a]	10.4778	0.10 ± 0.02	0.16	–	10.4759	–	0.18
	6	(10.6706)[a]	10.6575	0.09 ± 0.02	0.18	–	10.6548	–	0.21
	7	(10.7736)[a]	10.7674	0.11 ± 0.02	0.18	–	10.7634	–	0.23
	8	(10.8406)[a]	10.8338	0.12 ± 0.03	0.24	–	10.8363	–	0.21
	9	–	10.8842	–	0.20	–	10.8823	–	0.26
	10	–	10.9179	–	0.21	–	10.9161	–	0.28
	11	–	10.9430	–	0.21	–	10.9415	–	0.29
	...	...	...	–	...	...	...	...	...
	∞	11.0599	11.0599 [b]			11.0603 [b]	11.0603 [b]		
	n		$3s^2 3p^3(^2P^\circ)ns$	$[^1P^o]$			$3s^2 3p^3(^2P^\circ)nd$	$[\ ^1P^o]$	
$3s^2 3p^4\ ^1D_2$									
	3					10.741359[c]	10.7397	0.007	0.008
						10.741393[d]	–	0.007	–
	4	–		–		–	11.2587	–	0.30
	5	10.712359[a]	10.71400	2.03	2.03	–	11.6536	–	0.26
		10.712257[b]	–	2.03	–	–	–	–	–
	6	–	11.1675	–	2.02	–	11.8519	–	0.22
	7	–	11.4017	–	2.06	–	11.9688	–	0.16
	8		11.7017	–	–	–	–	–	–
	...		...	–	–	...	–	–	...
	∞		12.2598[b]	–	–	12.2598[b]	12.2598[b]		

[a] Experimental work from the thesis of Barthel [30].
[b] Rydberg series limits E_∞ for the sulfur ion (S^+) are from the NIST tabulations [67].
[c] NIST tabulations [67].
[d] Experimental work of Pan and co-workers [23].

different pulse energies of the laser photolysis produce different product distributions.

Note, a high photon density would lead to multi-photon effects, with a branching ratio that may differ significantly from that of one-photon excitation conditions. Pulse energies of 1-2 mJ/cm^2 [19] may cause additional contributions of $S(3s^2 3p^4\ ^3P)$ by the dissociation of vibrationally excited CS. The pulse energy of the 193

nm (6.424 eV) excitation radiation, used in the present work, is about 0.4 mJ/cm^2, so we safely assume that multi-photon effects play a minor role.

In Figure 5 the energies of the $^4S^o$, $^2D^o$ and $^2P^o$ thresholds for the S^+ ion relative to the S($3s^2 3p^4\ ^1D$) threshold are located at 9.215 eV ($^4S^o$), 11.060 eV ($^2D^o$), and 12.256 eV ($^2P^o$), respectively. These thresholds are indicated in Figure 5 by vertical dashed lines. It should be noted that direct photoionization is spin-forbidden in the $^4S^o$ - continuum because of the totality of the $^4S^o$-continuum and the emitted photoelectron.

In the energy range below 12.5 eV, autoionizing Rydberg series are observed, converging to the energetically higher lying ionic continua. These two allowed ionic continua $S^+(^2D^o)$ and $S^+(^2P^o)$ are located at 11.060 eV and 12.256 eV, respectively. A significant increase in photoionization efficiency is recorded above a photon energy of about 14.6 eV (c.f. Figure 4 (a)). There is a wide maximum structure stretching to about 17 eV with a shoulder at about 15.4 eV. This would appear to be due to residual molecular effects from the photolysis process, as outlined in Table I (cf. Section IV B). Evidence for this assumption comes from the fact that these features do not show up in the corresponding theoretical work on atomic sulfur from the excited $3s^2 3p^4\ ^1D_2$ metastable state as illustrated in Figure 4 (b). In the energy region below the $S^+(^2P^o)$ threshold the assignment of the resonance features in the photoionization spectra are in good agreement with those available in the literature. The respective Rydberg states couple via the process of autoionization to the ionic $^4S^o$ continuum. Between the individual resonances, the S^+ yield falls almost to zero.

The present study gives resonant structures assignment for the Rydberg series converging to the $S^+(^2D^o_{3/2,5/2})$ ionic thresholds. Autoionizing resonance states are observed for the main Rydberg series, converging to the $S^+(^2D^o)$ ionic continuum shown in Figure 5 (a) and (b). The most intense of the resonance series is the $3s^2 3p^3(^2D^o)nd\ ^1D^o$. Here, the transitions can be resolved for the n = 3, 4, 5, 6, 7, and 8 members of the Rydberg resonance series (see Table II). The higher members are not observed due to the low intensity and the limited experimental resolution of the VUV radiation. Theoretical predictions from the 512-level DARC calculations (given in Table II) are seen to be in good agreement with the experimental measurements and with the measurements of Pan and co-workers [23] (i.e., Series II). All the autoionizing Rydberg transitions occurring in atomic sulfur from the $3s^2 3p^4\ ^1D_2$ excited metastable state, at energies below the $^2D^o_{3/2,5/2}$ thresholds, are seen to be in good agreement with the values available from the literature [23, 67].

Rydberg series members are observed for the $3s^2 3p^3(^2D^o)ns\ ^1D^o$ resonances series with principal quantum numbers n = 5, 6, and 7. This series was also observed by Pan and co-workers [23] (i.e. Series I). We note that the n = 6 and n = 7 Rydberg members partially overlap. The resonance found at 10.59 ± 0.02 eV is from the $3s^2 3p^3(^2D^o)nd\ ^1P^o$ Rydberg series where $n = 6$. This transition appears unusually intense and there are no other members of this group observed. The unusually high intensity of this transition is due to the energetic proximity explained by the triplet Rydberg states and the interference with the singlet state.

In the present work we observe for the first time autoionizing Rydberg resonance states above the $^2D^o$ threshold and lying below the $^2P^o$ continuum. These resonances are also seen in the DARC photoionization cross section calculations for the ground and metastable states (see Figure 6). The excited Rydberg resonance states in the cases discussed so far are all $^1D^o$ and $^1P^o$ states. The ionic continuum to which these states couple in autoionization to is a $^4S^o$ continuum. The spin S_J of the ionic core is 3/2. Secondly, if one considers the totality of the ionic core and the emitted electron with spin $s = \pm 1/2$, a total spin S of 1 or 2 is possible. This will give rise to triplet and quintet-terms, while the autoionizing Rydberg states form singlet terms. Taking into account the selection rules for autoionization $\Delta S = 0$ appears initially banned for this transition. Under spin-orbit coupling we can expand the selection rule of the autoionization however, to $\Delta S = 0, \pm 1, \pm 2$. For transitions of this type, due to the spin-orbit coupling, large resonances appear having relatively narrow width.

The autoionization resonance occurs with a maximum at a photon energy of 10.11 ± 0.02 eV. However, it appears broadened and can be assigned to the $3s^2 3p^3(^2D^o)nd\ ^3D^o$ series. Here, for the process of autoionization, the selection rule $\Delta S = 0$ follows, as no spin-orbit coupling effects are involved. The lifetime will therefore be significantly reduced and the autoionization resonances appear much broadened. It should be noted that the excitation of the $3s^2 3p^4\ ^1D$ state in a $3s^2 3p^4\ ^3D$ Rydberg state to the spin-selection rule in the context of one-photon processes is contrary, illustrated by the relatively low intensity. This transition was also observed by Yang and co-workers [21, 22] who indicated that spin-spin and spin-orbit interactions in the case of atomic sulfur may play a role.

The autoionization resonance, located at a photon energy of 9.40 ± 0.02 eV, may be assigned to a known atomic transition of singlet sulfur. This structure was also observed by Pan and co-workers [23] at a wavenumber of 75 821 cm^{-1} (corresponding to 9.401 eV) and by Yang et al. [21, 22] for a wavenumber of 75 818 cm^{-1} (corresponding to 9.400 eV). Pan et al. [23] discussed an assignment to a ^1G series, but because of $\Delta J = 2$ this was excluded. Yang and co-workers [21, 22] suggested the transfer of excitation to a $3s^2 3p^3(^2D^o)3d$ state, without the corresponding term symbol. The energy of the photon ArF laser (6.42 eV) is insufficient to form atomic sulfur in the excited state S(^1S), since the photodissociation energy of CS_2 is 397 kJ/mol = 4.114 eV [76] and the excitation energy of S(^{1}S) is 2.7499637 eV [67] so that this electronic state is excluded as the cause of the resonance. The resonance lies energetically above the $^4S^o$

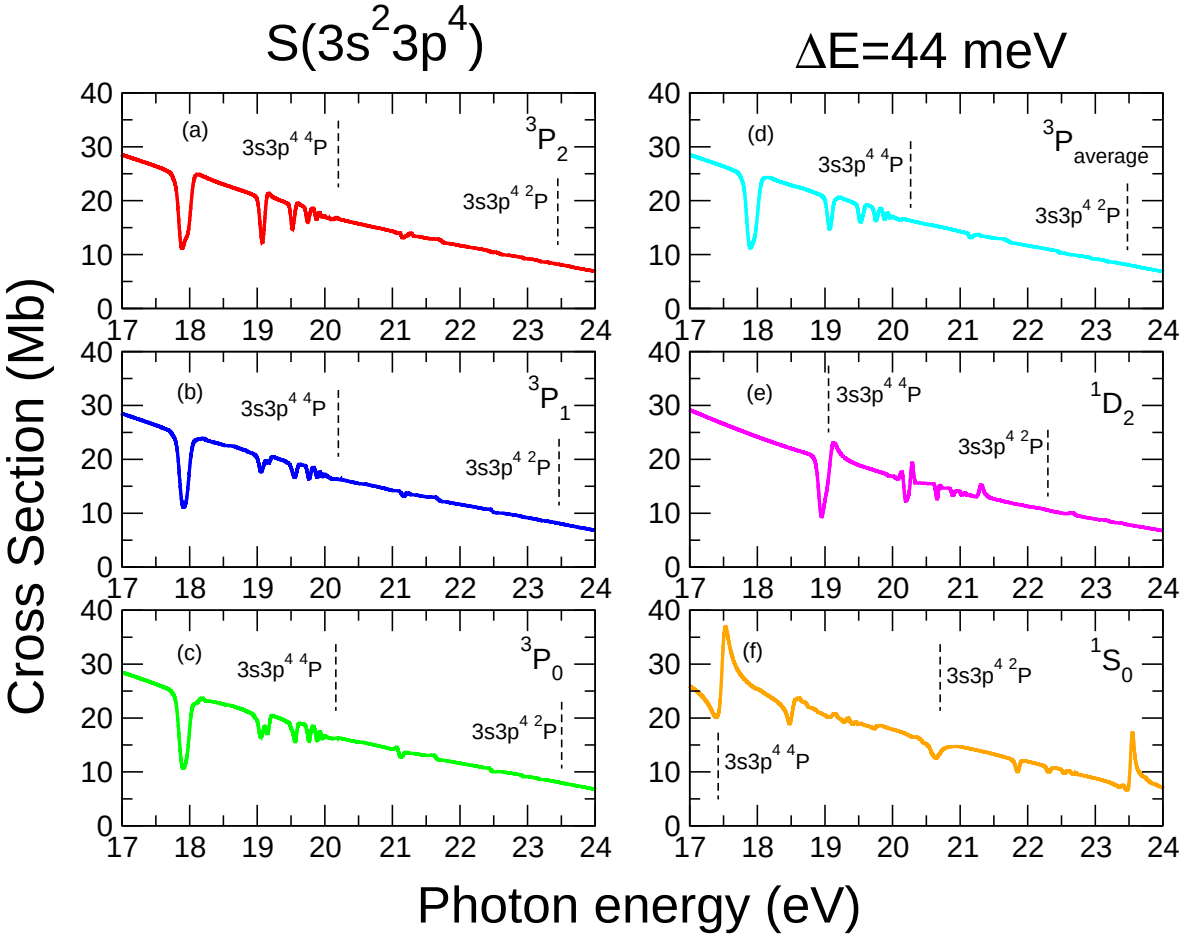

FIG. 7. (Color online) Theoretical cross sections results from the 512 level DARC for the sulfur $3s^2 3p^4\ ^3P_{2,1,0}$, and $3s^2 3p^4\ ^1D_2$, and $3s^2 3p^4\ ^1S_0$ initial states, in the photon energy region 17 – 24 eV, convoluted with a Gaussian having a profile of 44 meV. (a) $3s^2 3p^4\ ^3P_2$, (b) $3s^2 3p^4\ ^3P_1$ (c) $3s^2 3p^4\ ^3P_0$, (d) $3s^2 3p^4\ ^3P$ level averaged, (e) metastable $3s^2 3p^4\ ^1D_2$, and (f) metastable $3s^2 3p^4\ ^1S_0$ cross sections. In this energy region the prominent window resonances converging to the singly ionized sulfur ion threshold $3s3p^4\ ^4P$ (lowest vertical dashed line) are clearly visible in the cross sections. See text for further details.

continuum of S(^3P), so the resonance in the photoionization of the ground-state sulfur is not observed. Against this background and given the relatively low excitation energy of 9.40 ± 0.02 eV, tentatively assigning this feature to a $3s^2 3p^3(^2D^o)3d$ state appears straightforward.

Rydberg series converging to the $^2P^o$ continuum are observed to be members of the $3s^2 3p^3(^2P^o)nd\ ^1P^o$ and the $3s^2 3p^3(^2P^o)ns\ ^1P^o$ resonance series. The autoionizing $3s^2 3p^3(^2P^o)5s\,^1P^o$ resonance state occurs at an energy of 10.70 ± 0.02 eV, the $3s^2 3p^3(^2P^o)3d\ ^1P^o$ state at a photon energy of 10.75 ± 0.02 eV. These energies are in good agreement with the values from the NIST tabulations [67] of 10.7123 eV and 10.7414 eV. We note that both resonances were observed by Pan and co-workers [23]. The quantum defect μ of the $5s$ resonance at an energy of 10.70 ± 0.02 eV is 2.03, while that for the $3d$ resonance (at an energy of 10.75 ± 0.02 eV), is approximately zero. Extrapolating with the Rydberg formula using (see equation 2) and converting all quantities to eV one could straight forwardly locate further members of the Rydberg resonance series.

For the energy of the higher lying members of the $3s^2 3p^3(^2P^o)ns\ ^1P^o$ and the $3s^2 3p^3(^2P^o)nd\ ^1P^o$ resonance series, experimental values of approximately, 11.393 eV for the $3s^2 3p^3(^2P^o)6s\ ^1P^o$ state and 11.406 eV for the $3s^2 3p^3(^2P^o)4d\ ^1P^o$ state are obtained. These values agree well with the energies of the structures observed at 11.37 ± 0.02 eV and 11.40 ± 0.02 eV. For this reason we assign these resonances to the $3s^2 3p^3(^2P^o)6s\ ^1P^o$ and the $3s^2 3p^3(^2P^o)4d\ ^1P^o$ states. The resonance state located at an photon energy of 11.16 ± 0.02 eV is not available from the NIST tabulations [67] since in the en-

TABLE III. Principal quantum numbers n, resonance energies (eV), and quantum defects μ of the prominent $S(3s^2 3p^3[^2P^\circ])ns, nd$ Rydberg series seen in the $S(3s^2 3p^4\ ^1S_0)$ photoionization spectra converging to the $S^+(3s^2 3p^3[^2P^\circ])$ thresholds. The assignments are shown in Figure 8. The theoretical results were obtained from the 512-level DARC calculations performed within the Dirac Coulomb R-matrix approximation.

Sulfur (Initial state)		E_n (eV) (Expt)	E_n (eV) (Theory)	μ (Expt)	μ (Theory)	E_n (eV) (Expt)	E_n (eV) (Theory)	μ (Expt)	μ (Theory)
	n		$3s^2 3p^3(^2P^\circ)ns$	$[^1P^o]$			$3s^2 3p^3(^2P^\circ)nd$	$[^1P^o]$	
$3s^2 3p^4\ ^1S_0$									
	3	–	–	–	–	9.1366[a]	9.1361	0.004[a]	0.005
	4	–	–	–	–	–	–	–	–
	5	9.1075[a]	9.02574	2.033[a]	2.109	–	–	–	–
	6	–	9.75287	–	2.114	–		–	–
	7	–	10.0852	–	2.108	–		–	–
	8	–	10.2592	–	2.127	–		–	–
	9	–	10.3743	–	2.021	–			–
	10	–	–	–	–	–			–
	...	...	...	–	...	...	...	...	...
	∞	10.65363	10.65363[b]			10.65363[b]	10.65363[b]		

[a] Experimental work of Yang et al. [21].
[b] Rydberg series limits E_∞ for the sulfur ion (S^+) are from the NIST tabulations [67].

ergy range above the $^2D^o$ - threshold no singlet resonance states are listed. The photon energy of 11.291 eV is the closest lying triplet state, namely, $3s^2 3p^3(^2P^o)4d\ ^3P^o$. However, as illustrated in Figure 5 (b), the DARC cross section calculations in the region above the $S^+(^2D^o)$ - threshold and below the $S^+(^2P^o)$ - threshold, intense singlet resonance states are seen including shoulder resonances located at approximately similar positions (see Table II).

To the best of the authors knowledge the only experimental study from the $S(3s^2 3p^4\ ^1S)$ metastable state is that of the work of Yang et al. [22] where the $S(^1D)$ and $S(^1S)$ atoms are produced by 193 nm (6.424 eV) photodissociation of CS_2. As mentioned above, the photon energy of a 193 nm (6.424 eV) laser is insufficient to produce $S(^1S)$ from CS_2 photodissociation. The formation of atomic S in its ^1S state is likely connected with two-photon absorption processes. To complete our study on this system we performed large-scale DARC calculations on this metastable state for the photon energy range from threshold (7.61 eV) up to 30 eV. Figure 6 (f) shows the cross section for this metastable state as a function photon energy. Similar to the work presented earlier we have convoluted the theoretical cross sections with a Gaussian having a profile of 44 meV. Here again in the energy region below 12 eV (see Figures 8 (a) and (b)), strong resonance features are found in the cross section which will be discussed in the following Sections.

G. Resonances: $S(3s^2 3p^4\ ^1D$ and $^1S)$

The electronic configuration $ns^2 np^4$ belongs to the atomic species O ($n = 2$) and S ($n = 3$) which we use as the basis to interpret the present results. Due to the different principal quantum numbers these states will have different energies. However, in general the energies of the sulfur atom appear lower by several eV. In the following, the observed photoionization efficiency of the atomic structure in the singlet sulfur $S(3s^2 3p^4\ ^1D)$ are interpreted in the region around 17 eV.

If one compares the photoion yield of atomic sulfur with that of atomic oxygen, it is remarkable that in both cases, the respective electronic ground state $S(3s^2 3p^4\ ^3P)$ and $O(2s^2 2p^4\ ^3P)$ series of the autoionizing Rydberg transitions are observed converging to the respective ^4P-threshold at 20.20 eV (S^+) and 28.48 eV (O^+) relative to the electronic ground state. For the two electronically excited species $S(3s^2 3p^4\ ^1D)$ and $O(2s^2 2p^4\ ^1D)$ a broad autoionization resonance occurs at photon energies below the respective energetic position of the ^4P-continuum. In the case of sulfur $S(3s^2 3p^4\ ^1D)$ metastable state, it has a shoulder on the low energy side. The resonance in the case of the metastable atomic oxygen $O(2s^2 2p^4\ ^1D)$ state is a Coster-Kronig process and may be assigned to the $2s^2 2p^4\ ^1D \rightarrow 2s2p^5\ ^1P^o$ transition with subsequent autoionization. The analog $3s3p^5\ ^1P^o$ state of atomic sulfur occurs energetically at significantly lower energy of 8.95 eV relative to $S(3s^2 3p^4\ ^1D)$ state. This value is below the ionization energy and represents the reason why autoionization of this state is not observed.

The window resonance may be depicted by a Fano profile, leading to a profile index q of 0.21 ± 0.01, a half-

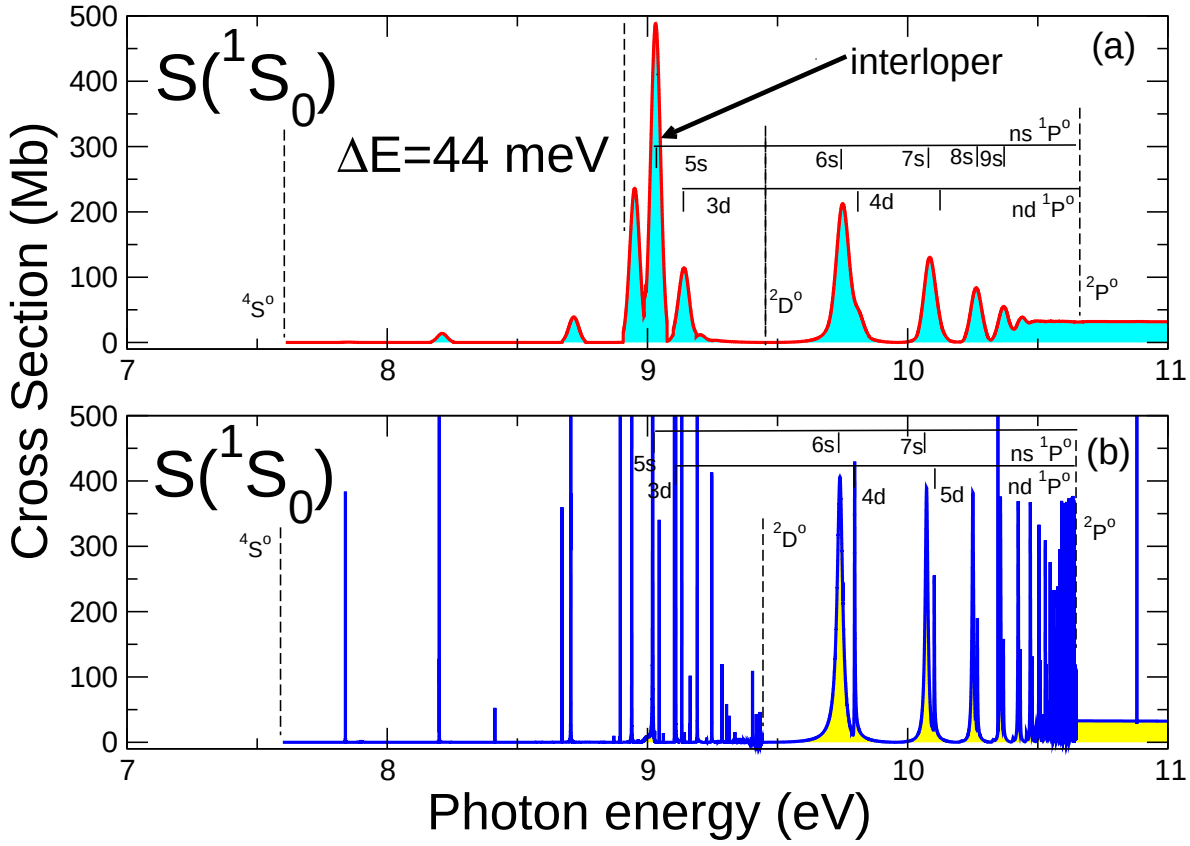

FIG. 8. (Color online) Single photoionization of atomic sulfur as a function of the photon energy in the $3s^2 3p^4\ ^1D$ metastable state from threshold to 12.5 eV. Theoretical cross section were carried out with the DARC codes, and convoluted with a Gaussian having a profile of 44 meV. The assigned Rydberg series are indicated as vertical lines grouped by horizontal or inclined lines. The corresponding series limits E_∞ of Equation 2 for each series are indicated by a vertical-dashed lines in the end of the line groups. The first few values of n for each series is displayed close to its corresponding vertical line in each group. Resonance energies and quantum defects for the various series are tabulated in Table II.

width Γ of 0.60 ± 0.005 eV located at an energy of 17.44 ± 0.006 eV. The observed intense structure in the experimental data is found at a photon energy of 16.92 ± 0.1 eV (c.f. Figure 4 (a)). An interpretation of this intense structure seen at 16.92 ± 0.10 eV may be given. We have already discussed that the $3s3p^5\ ^1P^o$ state is due to $3s$-valence excitation of atomic sulfur at higher excitation energies, an expected analog excitation of a $3s$-electron to the np orbitals with $n > 3$ can occur. The electron configuration in the case of inner-shell excitation $3s3p^4np$ forms a multiple of terms. Atomic sulfur has the terms ^3P, ^1D, ^1S resulting from the $3s^23p^4$ configuration. Term energies for the $3s$ excited states with the exception of the $3s3p^4np\ ^5P^o$ and $3s3p^4nd\ ^5D$ Rydberg series are unpublished, but calculations are available from the OPACITY project [84]. The ^5P-states can be considered as an indication that the appropriate $3s$ excited singlet terms with similar energies are expected. An intense autoionization resonance is observed at a photon energy of 16.92 ± 0.10 eV Although it may occur in the autoionizing Rydberg resonances below the $^2D^o$-continuum a resonance is observed, corresponding to a spin-forbidden $3s^23p^4\ ^1D$ transition, and assigned to a ^3D Rydberg state. However this resonance relative to the spin-allowed singlet-singlet transitions is significantly less intense.

A broad resonance is observed (c.f. Figure 4 (a)) with the peak at a photon energy of 16.92 ± 0.10 eV and the shoulder at 15.45 ± 0.10 eV, due to $3s^23p^4\ ^1D \rightarrow 3s3p^4np$ excitation associated with subsequent autoionization. The averaged half-widths are 0.55 ± 0.05 eV for

the state located at 15.45 ± 0.10 eV and 1.35 ± 0.25 eV for the state located at 16.92 ± 0.10 eV. These correspond to lifetimes of 1.20 ± 0.10 fs and 0.49 ± 0.08 fs, respectively. Both these values are larger than that of the corresponding atomic oxygen case which has an observed lifetime of 0.30 ± 0.02 fs for the $2s2p^5\ ^1P^o$ state.

As already indicated by the Fano profile indices q of the resonances located at 15.45 ± 0.10 eV and 16.92 ± 0.10 eV (see Figure 4 (a)), with lifetimes of 3.85 ± 0.42 fs and 2.15 ± 00.15 fs respectively. Both these states have lower values than the atomic oxygen case of 4.25 ± 0.80 fs. Accordingly, in the case of the smaller profile, the index q for sulfur indicates a less efficient coupling. At a photon energy of 16.92 ± 0.10 eV a broad autoionization resonance is observed with an absolute photoionization cross section of 23.6 ± 2.5 Mb and a shoulder at 15.45 ± 0.10 eV with a cross section value of 9.0 ± 1.2 Mb. The structures are due to $3s^23p^4\ ^1D \rightarrow 3s3p^4np\ ^1P^o,^1D^o,^1F^o$ transitions with $n > 3$. The fitted experimental data yield a Fano profile q value of 2.15 ± 0.15.

We note for the case of the $3s^23p^4\ ^1S$ metastable state, the $3s^23p^3(^2P^o)5s\ ^1P^o$ resonance state lies below the $S^+(^2D^o)$ threshold and is therefore an interloping resonance [73], as illustrated in Figure 8, which disrupts the regular Rydberg pattern. Above the $S^+(^2D^o)$ threshold region and below the $S^+(^2P^o)$ threshold the $3s^23p^3(^2P^o)ns\ ^1P^o$ series follows it normal Rydberg pattern as no interlopers are present. Only the lowest member $3s^23p^3(^2P^o)3d\ ^1P^o$ of the $3s^23p^3(^2P^o)nd\ ^1P^o$ resonance series was found. Our theoretical values for the positions and quantum defects are seen from Table III to be in suitable agreement with the measurements of Yang and co-workers [21]. The $3s^23p^3(^2P^o)3d\ ^1S^o$ resonance found by Yang and co-workers [21], located at 9.2035 eV, is forbidden by dipole selection rules in LS-coupling but shows up as a very faint resonance feature at approximately 9.2096 eV in our theoretical cross section.

V. DISCUSSION

Photodissociation of CS_2 at an excitation wavelength of 193 nm (6.424 eV) with subsequent photoionization of the neutral, formed photofragments in the photon energy range between 9.25 and 30 eV is reported. For atomic sulfur formed in the electronic states $S(3s^23p^4\ ^3P)$ and $S(3s^23p^4\ ^1D)$ measurements are performed up to 30 eV for both states. Autoionizing Rydberg resonances in the energy below 13.40 eV are observed and a detailed analysis is carried out for them.

Subtracting the proportion of $S(3s^23p^4\ ^3P)$ from the photo-ion yield curves above that of S^+ from $S(3s^23p^4\ ^3P)$ and $S(3s^23p^4\ ^1D)$, provides atomic triplet sulfur $S(^3P)$ from the photodissociation of S_2O for photon energies in the range 10.25 eV to 30 eV. This allows photoionization measurements to be made on the triplet state of atomic sulfur for photon energies over this photon energy range. For $S(3s^23p^4\ ^3P)$, autoionization resonances occurring in the experimental and theoretical investigations, i.e. in the photon energy range between 12 – 25 eV, intense window resonances are observed, that converge to the fourth ionization at 20.20 eV, as shown in Figure 2 and Figure 4 and illustrated more vividly in Figure 7.

Similarly, the photoion yield curve of electronically excited atomic sulfur $S(3s^23p^4\ ^1D)$ is determined by subtracting the amounts of $S(3s^23p^4\ ^3P)$ from the S^+ yield curves determined in the pump-probe experiments in the energy regime up to 30 eV for CS_2 molecule. Here, the first few members of the autoionizing Rydberg resonances series below the $^2D^o$ threshold (located at 11.06 eV) and the $^2P^o$ threshold (located 12.256 eV) are observed. At a photon energy of 16.92 ± 0.10 eV, a highly intense and a strongly broadened autoionization resonance is found. This resonance has a shoulder at 15.45 ± 0.10 eV and may be due to 3s-inner shell excitation. The large Auger width of 1.35 ± 0.25 eV for this resonance dominates the photoionization spectra of the electronically excited $S(3s^23p^4\ ^1D)$ in this photon energy region. Over the photon energy range 16 – 20 eV the cross section is dominated by remnants of the molecular precursors from the photolysis process. The origin of these processes is discussed in Section IV. A. This enhancement is not observed in the corresponding calculated atomic photoionization cross section so we conclude they are due to molecular effects.

VI. SUMMARY

The photoionization cross sections for atomic sulfur in the states $S(3s^23p^4\ ^3P)$ and $S(3s^23p^4\ ^1D)$, are an important basis for atmospheric and astrophysical models. Broad autoionizing resonances, observed in the case of electronically excited sulfur atoms are found by pump-probe experiments starting from molecular precursors. Numerous autoionization resonances are observed which facilitate the assignment of the sulfur species under study. Specifically, experimental measurements and large-scale photoionization cross sections calculations are presented for the ground and metastable states of atomic sulfur. A detailed analysis has been performed for the resonance features observed in the corresponding cross sections and the Rydberg series assigned spectroscopically. Below 13.5 eV similar resonance features are seen in the experimental measurements and the theoretical work, which have been analyzed and compared. Overall the resonance features observed in this photon energy region show suitable agreement between experiment and theory.

For the photon energy range 16 – 20 eV the experimental cross section is dominated by the remnants of the molecular precursor from the photolysis process not present in the theoretical calculations for this atomic species. The possible origin of these processes is discussed.

ACKNOWLEDGMENTS

Financial support by the German Research Foundation (DFG) is gratefully acknowledged (RU 420/7-1). B. M. McL. acknowledges support by the US National Science Foundation under the visitors program through a grant to ITAMP at the Harvard-Smithsonian Center for Astrophysics, Queen's University Belfast through a visiting research fellowship (VRF) and the hospitality of ER and the Physikalische Chemie Department of the Freie Universität of Berlin, during a recent research visit. This research used resources of the National Energy Research Scientific Computing Center, which is supported by the Office of Science of the U.S. Department of Energy (DOE) under Contract No. DE-AC02-05CH11231. The computational work was performed at the National Energy Research Scientific Computing Center in Oakland, CA, USA and at The High Performance Computing Center Stuttgart (HLRS) of the University of Stuttgart, Stuttgart, Germany. This research also used resources of the Oak Ridge Leadership Computing Facility at the Oak Ridge National Laboratory, which is supported by the Office of Science of the U.S. Department of Energy (DOE) under Contract No. DE-AC05-00OR22725.

[1] J. A. Cardelli, S. R. Federman, D. L. Lambert, and C. E. Theodosiou, Astrophys. J. **416**, L41 (1993).
[2] B. Sharpee, Y. Zhang, R. Williams, E. Pellegrini, K. Cavagnolo, J. A. Badwin, M. Phillips, and X. W. Lui, Astrophys. J. **659**, 1265 (2007).
[3] N. C. Sterling, H. L. Dinerstein, and T. R. Kallman, Astrophys. J. Suppl. Ser. **169**, 37 (2007).
[4] A. L. Broadfoot, B. R. Sandel, D. E. Shamansky, J. C. McConnell, G. R. Smith, J. B. Holberg, S. K. Atreya, T. M. Donahue, D. F. Strobel, and J. L. Bertaux, J. Geophys. Res. **86**, 8259 (1981).
[5] D. E. Shemansky and G. R. Smith, J. Geophys. Res. **86**, 9179 (1981).
[6] W. H. Symth and M. R. Combi, Astrophys. J. **328**, 888 (1988).
[7] M. E. Summers, D. F. Strobel, Y. L. Yung, J. T. Trauger, and F Mills, Astrophys. J. **343**, 468 (1989).
[8] R. R. Meier and M. F. A Hearn, Icarus **125**, 164 (1997).
[9] G. Pineau des Forêts, E. Roueff, and D. R. Flower, Mon. Not. Roy. Astron. Soc. **223**, 743 (1986).
[10] J. L. Kohl and W. H. Parkinson, Astrophys. J. **184**, 641 (1973).
[11] A. K. Dupree, Adv. At. Mol. Phys. **14**, 393 (1978).
[12] G. G. Lombardi, B. L. Cardon, and R. L. Kurucz, Astrophys. J. **248**, 1202 (1981).
[13] D. R. Garnett, Astrophys. J. **345**, 771 (1989).
[14] G. Tondello, Astrophys. J. **172**, 771 (1972).
[15] V. N. Sarma and Y. N. Joshi, Physica **123C**, 349 (1984).
[16] S. T. Gibson, J. P. Greens, B. Ruščić, and J. Berkowitz, J. Phys. B: At. Mol. Phys. **19**, 2825 (1986).
[17] N. Joshi, M. Mazzoni, A. Nencioni, W. H. Parkinson, and A. Cantu, J. Phys. B: At. Mol. Phys. **20**, 1203 (1987).
[18] V. Kaufman, Phys. Scr. **26**, 439 (1979).
[19] D. Xu, J. Huang, and W.M. Jackson, J. Chem. Phys. **120**, 3051 (2004).
[20] J. Huang, D. Xu, A. Stuchebrukhov, and W.M. Jackson, J. Chem. Phys. **122**, 144321 (2004).
[21] J. Zhou, B. Jones, X. Yang, W. M. Jackson, and C. Y. Ng, J. Chem. Phys. **128**, 014305 (2008).
[22] X. Yang, J. Zhou, B. Jones, C. Y. Ng, and W. M. Jackson, J. Chem. Phys. **128**, 084303 (2008).
[23] Wan-C Pan, I-Chia Chen, Tzu-P Huang, Jih-Y Yuh, and Yin-Y Lee, J. Chem, Phys. **129**, 1343305 (2008).
[24] R. Flesch, M. C. Schürmann, J. Plenge, H. Meiss, M. Hunnekuhl, and E. Rühl, Phys. Rev. A **62**, 052723 (2000).
[25] R. Flesch, A. Wirsing, M. Barthel, J. Plenge, and E. Rühl, J. Chem. Phys. **128**, 074307 (2008).
[26] B. Leroy, G. Le Bras, and P. Rigaud, Annales de Geophyquie **37**, 297 (1981).
[27] C. Y. R. Wu and D.L. Judge, Geophys. Res. Lett. **8**, 769 (1981).
[28] H. Xu and J.A. Joens, Geophys. Res. Lett. **20**, 1035 (1993).
[29] F. Z. Chen and C.Y.R. Wu, Geophys. Res. Lett. **22**, 2131 (1995).
[30] M. Barthel, *Photoionization of Atoms and Molecules in defined states* (PhD,thesis, Free University of Berlin, Berlin, Germany, 2009).
[31] G. Lakshminarayana, J. Mol. Spectrosc. **55**, 141 (1975).
[32] K.-E. J. Hallin, A. J. Merer, and D. J. Milton, Can. J. Phys. **55**, 1858 (1977).
[33] C. L. Chiu, P. C. Sung, and L. D. Chen, J. Mol. Spectrosc. **94**, 343 (1982).
[34] D. J. Clouthier, J. Mol. Spectrosc. **124**, 179 (1987).
[35] M. J. Conneely, K. Smith, and L. Lipsky, J. Phys. B: At. Mol. Phys. **3**, 493 (1970).
[36] C.Mendoza and C. J. Zeippen, J. Phys. B: At. Mol. Phys. **21**, 259 (1988).
[37] S. S. Tayal, Phys. Rev. A **38**, 729 (1988).
[38] C. T. Chen and F. Robicheaux, Phys. Rev. A **50**, 3968 (1994).
[39] Z. Altun, J. Phys. B: At. Mol. Opt. Phys. **25**, 2279 (1992).
[40] R. Flesch, M.-C. Schürmann, M. Hunnekuhl, H. Meiss, J. Plenge, and E. Rühl, Rev. Sci. Instrum. **71**, 1319 (2000).
[41] I. C. E. Turcu and J. B. Dance, *X-Rays from Laser Plasmas: Generation and Applications* (Wiley, Chichester, 1998).
[42] J. Plenge, R. Flesch, M. C. Schürmann, and E. Rühl, J. Phys. Chem. A **105**, 4844 (2001).
[43] R. Flesch, J. Plenge, M. C. Schürmann, S. Kühl, M. Klusmann, and E. Rühl, Surf. Rev. Lett. **9**, 105 (2002).
[44] J. Plenge, R. Flesch, S. Kühl, B. Vogel, R. Müller, F. Stroh, and E. Rühl, J. Phys. Chem. A **108**, 4859 (2004).
[45] J. Berkowitz, *Photoabsorption, Photoionization and Photoelectron Spectroscopy* (Academic, New York, 1979).
[46] L.-E. Berg, P. Erman, E. Kallne, S. Sorensen, and G. Sundstrom, Phys. Scr. **44**, 328 (1991).
[47] W.C. Wiley and I.H. McLaren, Rev. Sci. Instrum. **26**, 1150 (1955).

[48] E. Rühl, C. Schmale, H.W. Jochims, E. Biller, M. Simon, and H. Baumgärtel, J. Chem. Phys. **95**, 6544 (1991).

[49] P.W. Schenk and R. Steudel, Z. Anorg, Allg. Chem. **342**, 253 (1966).

[50] P.W. Schenk, R. Steudel, and M. Töpfert, Z. Naturforsch. **19b**, 535 (1964).

[51] P.W. Schenk and R. Steudel, Angew. Chem. **76**, 97 (1964).

[52] J. A. R. Samson, *Vacuum ultraviolet spectroscopy* (Wiley, Chichester, 1967).

[53] P. H. Norrington and I. P. Grant, J. Phys. B: At. Mol. Opt. Phys. **20**, 4869 (1987).

[54] W. P. Wijesundera, F. A. Parpia, I. P. Grant, and P. H. Norrington, J. Phys. B: At. Mol. Opt. Phys. **24**, 1803 (1991).

[55] DARC codes URL, `http://web.am.qub.ac.uk/DARC`, `http://connorb.freeshell.org`.

[56] C. P. Ballance and D. C. Griffin, J. Phys. B: At. Mol. Opt. Phys. **39**, 3617 (2006).

[57] B. M. McLaughlin and C. P. Ballance, J. Phys. B: At. Mol. Opt. Phys. **45**, 095202 (2012).

[58] B. M. McLaughlin and C. P. Ballance, J. Phys. B: At. Mol. Opt. Phys. **45**, 085701 (2012).

[59] V. Fivet, M. A. Bautista, and C. P. Ballance, J. Phys. B: At. Mol. Opt. Phys. **45**, *035201* (2012).

[60] G. Hinojosa, A. M. Covington, G. A. Alna'Washi, M. Lu, R. A. Phaneuf, M. M. Sant'Anna, C. Cisneros, I. Álvarez, A. Aguila, A. L. D. Kilcoyne, A. S. Schlachter, C. P. Ballance, and B. M. McLaughlin, Phys. Rev. A **86**, 063402 (2012).

[61] A. Müller, S. Schipper, D. Esteves-Macaluso, M. Habbi, A. Aguilar, A. L. D. Kilcoyne, R. A. Phaneuf, C. P. Ballance, and B. M. McLaughlin, J. Phys. B: At. Mol. Opt. Phys. **47**, 215202 (2014).

[62] E. T. Kennedy, J. -P. Mosnier, P. Van Kampen, D. Cubaynes, S. Guilband, C. Blancard, B. M. McLaughlin, and J. M. Bizau, Phys Rev. **90**, 063409 (2014).

[63] P. C. Ohja and A. Hibbert, J. Phys. B: At. Mol. Opt. Phys. **22**, 1153 (1989).

[64] F. P. Keenan, P. C. Ohja, and A. Hibbert, Phys. Scr. **48**, 129 (1993).

[65] B. M. McLaughlin, and C. P. Ballance, in *Sustained Simulated Performance 2014*, Chapter 15, edited by M. Reich, Y, Kovalenko, E. Focht, W. Bez, and H. Kobaysahi (Springer, New York and Berlin, 2014).

[66] B. M. McLaughlin, C. P. Ballance, M S Pindzola, and A Müller, in *High Performance Computing in Science and Engineering 2014*, Chapter 4, edited by W. E. Nagel, D. B. Kröner, and M. Reich (Springer, New York and Berlin, 2014).

[67] Y. Ralchenko, A. E. Kramida, J. Reader, and NIST ASD Team, "NIST Atomic Spectra Database (version 5)," National Institute of Standards and Technology, Gaithersburg, MD, USA.

[68] J. Sugar and A. Musgrove, J. Phys. Chem. Ref. Data **20**, 859 (1991).

[69] E. B. Saloman, J. Phys. Chem. Ref. Data **36**, 215 (2007).

[70] M. J. Seaton, Rep. Prog. Phys. **46**, 167 (1983).

[71] L. Quigley and K. A. Berrington, J. Phys. B: At. Mol. Opt. Phys. **29**, 4529 (1996).

[72] L . Quigley, K. A. Berrington, and J. Pelan, Comput. Phys. Commun. **114**, 225 (1998).

[73] C. P. Ballance, K. A. Berrington, and B. M. McLaughlin, Phys. Rev. A **60**, R4217 (1999).

[74] P. Coppens, J. C. Reynaert, and J. Drowart, J. Chem. Soc. Faraday Trans. **75**, 292 (1979).

[75] W.C. Martin, R. Zalubas, and A. Musgrove, J. Phys. Chem. Ref. Data **19**, 821 (1990).

[76] B. deB. Darwent, *Bond Dissociation Energies in Simple Molecules* (National Bureau of Standards NSRDS-NBS 31, Washington D C, USA, 1970).

[77] F. Innoecenti, L. Zuin, M. L. Costa, A. A. Dias, A. Morris, S. Stranges, and J. M. Dyke, J. Chem. Phys. **126**, 154310 (2007).

[78] J. J. Yeh and I. Lindau, At. Data Nucl. Data Tables **32**, 1 (1985).

[79] J. Berkowitz, G. B. Ellison, and D. Gutman, J. Phys. Chem. **98**, 2744 (1994).

[80] G. C. Angel and J. A. R. Samson, Phys. Rev A **38**, 5578 (1988).

[81] J. Berkowitz, C. H. Batson, and G. L. Goodman, Phys. Rev. A **24**, 149 (1981).

[82] F. Qi, L. Sheng, M. Ahmed, D. S. Peterka, and T. Baer, Chem. Phys. Letts. **357**, 204 (2002).

[83] I. M. Waller and J. W. Hepburn, J. Chem. Phys. **87**, 3261 (1987).

[84] The Opacity Project Team, *The Opacity Project Vol. 1* (Institute of Physics Publications, Bristol,UK, 1995).